Case Study

Evaluation of Satellite and Gauge-Based Precipitation Products through Hydrologic Simulation in Tigris River Basin under Data-Scarce Environment

Aws A. Ajaaj[1]; Ashok K. Mishra, M.ASCE[2]; and Abdul A. Khan, F.ASCE[3]

Abstract: This study investigates four widely used satellite and gauged-based precipitation products for hydrological evaluation in the poorly gauged Tigris River basin (TRB), with an area of 445,656 km^2, using the Soil and Water Assessment Tool (SWAT) watershed model. The multiple precipitation data sources (PDSs) evaluated in this study include Precipitation Estimation from Remotely Sensed Information using Artificial Neural Networks-Climate Data Record (PERSIANN-CDR), Multisource Weighted-Ensemble Precipitation (MSWEP), Asian Precipitation Highly Resolved Observational Data Integration towards the Evaluation of water resources project (APHRODITE), and National Oceanic and Atmospheric Administration (NOAA) Climate Prediction Center (CPC) data. The SWAT model was calibrated using three approaches to identify more realistic parameters. Overall, APHRODITE could capture the spatiotemporal distributions of daily precipitation with a correlation coefficient of 0.65, root-mean square error of 0.62 mm, and percent bias of 19.1%. In addition, APHRODITE also captured the monthly streamflow with reasonably accuracy for selected streamflow stations in the TRB with mean Nash-Sutcliffe efficiency of >0.65. Conversely, MSWEP overestimated and CPC underestimated the observed mean climatology, respectively, and had similar effects on monthly streamflow simulations. Among all the selected precipitation products, the relative performance of CPC is poor in comparison to other data sets. **DOI: 10.1061/(ASCE)HE.1943-5584.0001737.**

Author keywords: Precipitation; Spatiotemporal variability; Soil and water assessment tool (SWAT); Remote sensing data.

Introduction

Hydrological models are useful tools for investigating hydrological processes in watersheds with limited actual measurements (Abbaspour et al. 2015; Amisigo et al. 2008; Li et al. 2009). Precipitation is one of the important inputs for hydrological models that are used to study surface and subsurface water flow and drought analysis in any watershed (Beven 2011; Miao et al. 2015). The availability of precipitation estimates from multisource data (i.e., satellite and radar data, interpolated from actual observations, or a combination of all) extended the application of hydrological models to areas where the actual observations are scarce. However, the quality, reliability, and the spatiotemporal variability of these precipitation data sources (PDS) need validation prior to their sectorial applications. Failure in representing the accurate spatiotemporal variability of precipitation may lead to errors and uncertainties in stream flow predictions especially in basins poorly represented by an actual rain gauge network (Andréassian et al. 2012; Faurès et al. 1995; Mishra and Singh 2010; Taesombat and Sriwongsitanon 2009). Therefore, it is important to validate the ability of a hydrological model driven by various PDSs to simulate the actual streamflow information for a specific region, especially with scarce data environment and to evaluate the errors associated with each PDS (Yang et al. 2015). For this purpose, the Soil and Water Assessment Tool (SWAT) (Arnold and Fohrer 2005) is utilized in this study due to its effectiveness in evaluating water quantity and quality (Gassman et al. 2007).

In many studies, multisource precipitation products are evaluated and validated against in situ precipitation for streamflow simulation using hydrological models (Behrangi et al. 2011; Karakoc and Patil 2016; Tobin and Bennett 2009; Yuan et al. 2017). Among many primary sources of precipitation estimates (e.g., surface network, ground-based radar, and satellite remote sensing retrieval), the remotely sensed satellite measurements have produced many high spatial (<4 km) and temporal (<3 hours) resolution precipitation products (Behrangi et al. 2014; Sorooshian et al. 2000). Several studies have evaluated the performance of satellite-based precipitation products for hydrologic applications in data sparse regions (Behrangi et al. 2014; Jiang et al. 2014; Lee et al. 2015; Tobin and Bennett 2011). For example, Thiemig et al. (2013) and Zhu et al. (2016) validated the use of satellite precipitation data for streamflow simulation and reported that using two satellite-based precipitation products, namely Tropical Rainfall Measurement Mission (TRMM) and Precipitation Estimation from Remotely Sensed Information using Artificial Neural Networks-Climate Data Record (PERSIANN-CDR), performed better in comparison to the reanalysis gauged-based data. Many studies have concluded that satellite-based precipitation products could be potentially used for hydrological predictions particularly for ungauged basins (Jiang et al. 2012; Xue et al. 2013).

The uncertainty associated with hydrological models, especially when using different model inputs, greatly affects the model performance. This may lead to less meaningful and sometimes misleading predictions if such uncertainties are not addressed in the calibration process (Schuol and Abbaspour 2006; Vrugt and Bouten 2002; Yang et al. 2007a, b). During model calibration, instead of relying on a single model prediction, statistical methods are used to

[1]Graduate Student, Glenn Dept. of Civil Engineering, Clemson Univ., 131G Lowry Hall, Clemson, SC 29634-0911. Email: aajaaj@g.clemson.edu

[2]Associate Professor, Glenn Dept. of Civil Engineering, Clemson Univ., 202A Lowry Hall, Clemson, SC 29634-0911 (corresponding author). Email: ashokm@g.clemson.edu

[3]Professor, Glenn Dept. of Civil Engineering, Clemson Univ., 218 Lowry Hall, Clemson, SC 29634-0911. Email: abdkhan@g.clemson.edu

Note. This manuscript was submitted on July 5, 2017; approved on August 9, 2018; published online on December 21, 2018. Discussion period open until May 21, 2019; separate discussions must be submitted for individual papers. This paper is part of the ***Journal of Hydrologic Engineering***, © ASCE, ISSN 1084-0699.

represent uncertainties in hydrological models, where such uncertainties are given a probabilistic range to account for several sources of errors in the model (Franz et al. 2010). These errors can be due to four major sources related to model inputs, structure, parameters, and output calibration data. The simplest statistical method for parameter reducing uncertainty is the first-order approximation, which uses a linear objective function. This approach does not account for correlation between model parameters (Vrugt and Bouten 2002). More complex algorithms such as sequential uncertainty fitting (SUFI), Monte Carlo-based algorithms, and Markov chain Monte-Carlo (MCMC) have been successfully applied to provide improved meteorological and hydrological predictions as well as to represent uncertainties in hydrological model parameters (Bates and Campbell 2001; Blasone et al. 2008; Gallagher and Doherty 2007). Although SUFI optimization method requires a massive number of simulations, it is very robust in predicting the parameters uncertainty and the corresponding streamflow simulations (Abbaspour et al. 1997, 2004), and therefore this method was applied in this study.

For the last few decades there has been a significant increase in water scarcity in the lower Tigris River basin (LTRB). This is highly attributed to the intense water management practices (including dam constructions, irrigation systems, and meeting drinking water demands) implemented in the upper Tigris River basin (UTRP), located in Turkey and Iran (Bozkurt and Sen 2011; Issa et al. 2014; Voss et al. 2013; Wilson 2012). The analysis of water resources in such watershed is challenging due to the scarcity of observed precipitation data caused by the ongoing conflicts and political instability (Marghany et al. 2016).

Motivated by the growing water demand in TRB as well as the availability multiple of precipitation products to support water management, the present study will investigate the following: (1) the spatiotemporal heterogeneities of the four PDSs [namely, Asian Precipitation Highly Resolved Observational Data Integration Towards the Evaluation of water resources project (APHRODITE), Multisource Weighted-Ensemble Precipitation (MSWEP), National Oceanic and Atmospheric Administration's (NOAA's) Climate Prediction Center (CPC), and PERSIANN-CDR] compared to actual gauge data over the TRB; (2) to evaluate the suitability of using these PDSs to simulate streamflow in such a large river basin with limited hydroclimate information; and (3) the predictive uncertainty of daily precipitation data was investigated for simulating streamflow. The results of this study will provide an insight into the importance of validating multiple PDSs for hydrological modeling when precipitation data are inadequate or unavailable.

Study Area

This study was conducted on the Tigris River basin [Fig. 1(a)], which encompasses a total drainage area of around 445,656 km^2, of which 56.1% is in Iraq, 24.5% in Turkey, 19% in Iran, and 0.4% in Syria (Rohstoffe 2013). The TRB has nine major tributaries, most of which originate in Turkey and Iran, and eventually meet Tigris River in Iraq (Frenken 2009; Shahin 2007). Approximately 30% of the TRB land is covered by intense agricultural areas [Fig. 1(b)], 26% is primarily covered with grassland, 35% is arid land, and the remaining 9% represents settlements in the basin (Kibaroğlu 2002). Based on the Digital Elevation Map (DEM) of the area, the topography of the TRB is highly variable where the elevation ranges from few meters in the south (lowlands) to 4,356 m above the sea level in the northeast (highlands).

The TRB is characterized by its transitional climate from semihumid in the headwaters (highlands) to semiarid (lowlands) (Ajaaj et al. 2016). The resulting change in elevation from the north to the south creates a strong spatial distribution of precipitation in the TRB. Most of the rain occurs between November and April, reaching maximum during winter months (December–February). The rest of the year (May–October) is dry particularly from June to August. Because most of the winter precipitation occurs in the mountains (UTRB), it is mostly stored as snow pack. Therefore, the resulting flow of the Tigris River is seasonal and dominantly relies on snowmelt during spring season, March–May (Jones et al. 2008). Given the semiarid climate of the LTRB, the evaporation causes a considerable loss of water from this part of the basin. Mean air temperature ranges from −35°C in winter (mountains) to 40°C in summer (Mesopotamian plain in the south of the TRB) (Rohstoffe 2013).

In the mid-1970s a general regional water resources plan was implemented in the UTRB aimed at increasing water withdrawal for agricultural, industrial, and municipal water supply (Tigrek and Kibaroglu 2011). Consequently, a progressive reduction in the flow of the Tigris River has been noticed in the LTRB, especially during dry season months (May–October). This has resulted in a loss of about 25% of the irrigated areas and drying up of most of the marshlands in the LTRB (Jones et al. 2008). For example, the mean annual flow rate at Kut station (southern LTRB) has been reduced by 50 m^3 s^{-1} from 1931–1973 to 1974–2004. The mean annual precipitations over the entire river basin for these two time periods are similar (473.34 and 472.80 mm, respectively), which makes the LTRB vulnerable to extreme drought under such management plans (Issa et al. 2014; Wilson 2012).

Hydrological Model

SWAT is a popular hydrological and water quality model developed by the USDA-Agricultural Research Service (USDA-ARS). It is a long-term, lumped, continuous, watershed-scale simulation model designed to assess the impact of different management practices on surface water, sediment, and agricultural chemical yields on a subbasin scale (Arnold and Fohrer 2005). The watershed in SWAT is classified into multiple subbasins that are further divided into unique combinations of land use, soil type, and slope known as hydrologic response units (HRUs). SWAT performs its calculations for each HRU then scales it back to subbasins based on the percentage of each HRU in that subbasin (Wible 2014). This hydrological model is based on a water balance equation (Arnold et al. 1998) as given by Eq. (1). In this equation, SW_t is the soil water content at time t; SW_o is the initial soil water content; and R, Q, ET, P and QR are the precipitation, runoff, evapotranspiration, percolation, and return flow, respectively, all measured in millimeters and at the time t in the day

$$SW_t = SW_o + \sum_{t=1}^{n}(R - Q - E - P - QR) \tag{1}$$

SWAT commonly uses two methods to estimate the surface runoff and infiltration including the Soil Conservation Service (SCS) and the Green-Ampt infiltration method, respectively. In this study, the SCS curve number method is chosen to model surface runoff in SWAT model. Three methods are used to simulate evapotranspiration in SWAT model including Penman-Monteith, Priestley-Taylor, and Hargreaves. Penman-Monteith is used in this study as it counts for wind speed, air temperature, relative humidity, and different land uses (Arnold et al. 2012), and has shown good empirical simulations (Earls and Dixon 2008). In SWAT, the snow is simulated as an equivalent depth of water, and the precipitation within an HRU is classified as snow if the mean air temperature drops below the snowmelt temperature threshold, which is determined through

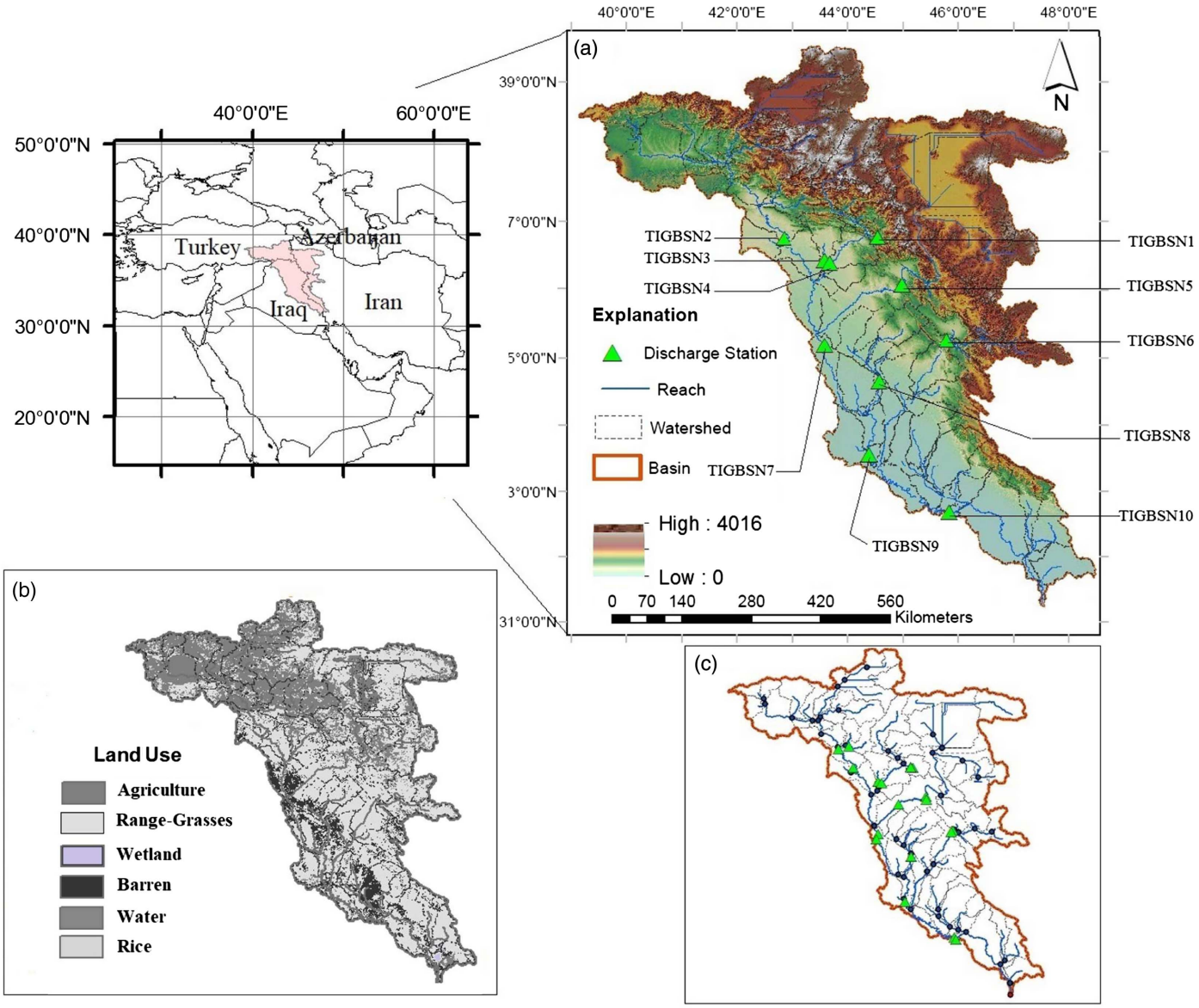

Fig. 1. Tigris River Basin location map: (a) DEM with stream gauges; (b) land use map; and (c) subbasins with outlets.

calibration. The subsurface system in SWAT is modeled as two components, shallow and deep aquifers. The shallow aquifer receives water from the unsaturated soil profile with a delay estimated using an exponential delay function, while only a fraction of the total recharge can percolate to the deep aquifer (Arnold and Fohrer 2005). SWAT model routes surface water as a volume through the channel network using either the variable storage routing method or the Muskingum routing method (used in this study).

Model Inputs for SWAT Model

Land use data for the year 2000 was derived from maps provided by European Commission Joint Research Center for Central Asia (Tateishi et al. 2011). Soil map for the study area was obtained from the global digital soil map provided by Food and Agricultural Organization of the United Nations (FAO 2013). A DEM at 90 m resolution is obtained from the Shuttle Radar Topography Mission (SRTM). This DEM is used to delineate the watershed. All of the meteorological inputs (i.e., temperature, wind, humidity, and solar radiation) except precipitation was obtained from the National Centers for Environmental Prediction (NCEP) and Climate Forecast System Reanalysis (CFSR) data set (Dile and Srinivasan 2014; Fuka et al. 2014). The data covers many years of records from 1979 onward on a daily basis and it has been updated for the current state of atmosphere.

Monthly streamflow data for multiple gauging stations located on Tigris River and its tributaries were obtained from the United States Geological Survey (USGS) Saleh 2010). A total of 10 stations were found reliable for use in calibration and validation of SWAT model. Table 1 summarizes the primary characteristics of these gauging stations for which streamflow was evaluated. The selected gauge stations represent two climate regimes (semi-humid and semiarid). The discharge data was examined and validated for missing data. If the flow rate was missing in any month, the mean flow rate of the two forward and two backward months was substituted for the missing month.

Precipitation Data

This section provides an overview of the major characteristics of the precipitation data sources considered in this study. Four grid-based daily precipitation data derived from multiple sources (historical

Table 1. Selected streamflow gauging stations located in Tigris River basin

River name and station location	Station ID	Latitude (degrees)	Longitude (degrees)	Drainage area (km^2)	Mean monthly discharge ($m^3 s^{-1}$)
Tigris River at Mosul	TIGBSN1	36.63	42.82	54,900	460.83
Greater Zab River at Bakhem	TIGBSN2	36.64	44.50	383	382.78
Khazir River at Manquba	TIGBSN3	36.30	43.55	2,900	31.20
Greater Zab River at Eski-Kelek	TIGBSN4	36.27	43.65	20,500	425.53
Lesser Zab River at Doka	TIGBSN5	35.95	44.95	233	233.36
Adhiam River at Fatha	TIGBSN6	35.05	43.55	107,600	767.04
Tigris River Injana	TIGBSN7	34.50	44.52	9,840	33.14
Diyala River at Derbindi-Khan	TIGBSN8	35.13	45.75	17,800	154.00
Tigris River at Baghdad	TIGBSN9	33.41	44.34	134,000	479.20
Tigris River at Gharraf	TIGBSN10	32.53	45.79	150,964	208.45

observations, radar, satellite, or a combination of the three) were used as input in SWAT model to simulate the observed monthly stream flow in the TRB. In addition, we included one actual gauge-based precipitation dataset to provide a realistic range of model parameters and to account for model uncertainty due to different precipitation inputs. The following subsections provide an overview of precipitation products used in this study.

The Asian Precipitation Highly Resolved Observational Data Integration towards the Evaluation of Water Resources project (Yatagai et al. 2012) is a product from the Research Institute for Humanity and Nature (RIHN) and the Meteorological Research Institute of Japan Meteorological Agency (MRI/JMA). This precipitation data product is interpolated from rain gauges and available for continental Asia including Himalayas, Southeast Asia, and mountainous areas of the Middle East for the period 1951–2007. This study uses the current version (V1101R1) of the data with a spatial resolution of 0.25° that covers the entire TRB domain.

Multisource Weighted Ensemble Precipitation is a recent global daily precipitation dataset with 0.25° grid spatial resolution and available for the period 1979–2015. MSWEP (Beck et al. 2017) combines data from satellite and both reanalysis and observed precipitation. The MSWEP data was further corrected for gauge-under catch and orographic errors by inferring catchment average precipitation from the streamflow data for 13,762 stations globally.

The National Ocean and Atmospheric Administration Climate Prediction Center (Xie et al. 2007) is based on the daily global precipitation data from multiple sources and it is available for the period 1979–2005 at 0.5° grid resolution. The CPC data is developed to create a precipitation database by combining precipitation from radar, satellite and over 30,000 rain gauge stations data across the globe.

PERSIANN-CDR data set is a multi-retrospective satellite-based data precipitation, consistent, long-term data that is used for hydrological studies and available for the period 1983–2016 at a spatial resolution of 0.25° in latitude band (60S-60N). The major advantages of PERSIANN-CDR data set are as follows: (1) this product provides consistency and long-term availability with more than 30 years updated quarterly; (2) it is derived from multiple data sources, which makes it more reliable; and (3) the high resolution monthly precipitation data set is consistent with GPCP monthly estimates (Ashouri et al. 2015; Knapp 2008; Sorooshian et al. 2000). The PERSIANN-CDR product is first developed by incorporating GridSat-B1 infrared satellite data into the PERSIANN algorithm and then is validated with the National Centers for Environmental Prediction (NCEP) Stage IV hourly precipitation data. The product is further adjusted using the Global Precipitation Climatology Project (GPCP) monthly product version 2.2 (GPCPv2.2) (Ashouri et al. 2015).

The actual daily gauge-based precipitation data (APD) was obtained from approximately 33 stations located in the TRB for the period 1957–1963 (the data is scarce and difficult to access). The continuity and the quality of this data source were examined; it was found that the daily data was not consistently documented for some gauge stations each month. Thus, the following steps were taken to generate APD gauge-based data: (1) for each month, the original stations were remapped (regridded) to a new uniform mesh grid defined on 0.25° longitude and latitude spatial resolution, and (2) precipitation at those new grid locations was evaluated using kriging interpolation method. The kriging technique is recommended for interpolating daily precipitation over deterministic methods (Ly et al. 2013).

Methodology

Model Setup and Calibration

ArcSWAT 2012 (Arnold et al. 2013) was used in this study. The delineation of the watershed and streams network was done based on the DEM (90 m resolution), which resulted in 99 subbasins for the TRB [Fig. 1(c)]. The subbasins were further divided into 5371 HRUs based on unique combinations of soil, land use, and slope. The Sequential Uncertainty Fitting-2 (SUFI-2), available in the SWAT-CUP package (Abbaspour et al. 2015) was used for model calibration and validation. The SUFI-2 algorithm maps all model parameter uncertainties and expresses them as a range of uniform distributions that account for all sources of uncertainties in the hydrological model (Abbaspour et al. 2004). A set of 22 flow parameters along with their range was identified for this process to determine the most sensitive parameters. Initial parameter ranges were assigned from large-scale SWAT models developed for neighboring areas and from tabulated parameter values in SWAT manual (Faramarzi et al. 2009). A full list of these parameters along with their default ranges is shown in Table 2. The sensitivity of the selected parameters was found using a global sensitivity analysis tool known as LH-Oah, which combines Latin hypercube sampling and one-factor-at-a-time sampling (Van Griensven et al. 2006).

In general, model parameters are usually sensitive with respect to change in the precipitation data source used in the hydrological model. Besides, different models forcing data could result in similar stream flow predictions after optimizing different parameters. Therefore, parameter sensitivity analysis of SWAT model for each of the fours PDSs and APD was conducted by applying three approaches for selection of parameters as follows, and Fig. 2 shows the flowchart of these techniques used for the parameters calibration process:

- Cumulative ranked parameter set (CRPS): The parameters obtained from SWAT model with each of the PDS as forcing precipitation input were ranked from 1 to 22 (with 1 being the most sensitive parameter). The mean of the four ranks from all PDS was determined to represent an overall cumulative rank (or CRPS) shown in Table 3. Top eight most sensitive parameters were identified using this procedure and the other 14 parameters were given default values. Final parameter ranges obtained from the CRPS approach assures comparing similar model parameters from estimated and observed precipitation. Strauch et al. (2012) used a similar procedure for calibrating SWAT model using five precipitation data sets.
- Gauge ranked parameter set (GRPS): The eight most sensitive parameters from SWAT model run with actual gauge precipitation data were identified. Then this set of parameters was used to calibrate SWAT model for streamflow for each of the PDSs. This procedure is termed as gauge ranked parameter set. This fixed parameter set procedure may have better representation for the hydrological conditions in the TRB and similar approach was earlier applied by Jiang et al. (2012).
- Individual ranked parameter set (IRPS): SWAT model is calibrated individually with each of the PDSs and labeled as individual ranked parameter set. The IRPS allows selecting the eight most sensitive parameters for each PDS independently in model calibration and validation. This method is different from CRPS because it allows SWAT model with each PDS to be calibrated independently (i.e., four parameter sets are identified in this process, one for each PDS).

Model Uncertainty and Performance Measures

In SUFI-2, the propagation of uncertainties in the hydrologic model parameters leads to uncertainties in model output variables such as streamflow. These uncertainties are usually expressed as probabilistic predictions calculated at 2.5% and 97.5% levels of the cumulative distribution of the output variables, which is also known as 95% prediction probability uncertainty (95PPU) (Abbaspour et al. 2015). Two statistical based factors, known as p-factor and r-factor, are commonly used to quantify uncertainties in simulated results (expressed as lower and upper bands of the 95PPU). The p-factor (>70% is acceptable value) is the percentage of the observed data bounded by upper and lower model outputs, while r-factor (around 1 is acceptable value) is the thickness of that band (Abbaspour et al. 2007). The r-factor is given by Eq. (2). Where the term $y_{t,97.5\%} - y_{t,25\%}$ includes the upper and the lower bounds of 95PPU at time t, and σ_{obs} is the standard deviation of the observed data sample

$$r - \text{factor} = \frac{\frac{1}{n}\sum_t^n (y_{t,97.5\%} - y_{t,25\%})}{\sigma_{obs}} \tag{2}$$

Model streamflow outputs are evaluated using multiple statistical criteria including correlation coefficient (CC), root-mean square error (RMSE), percent bias (PBIAS), and Nash-Sutcliffe efficiency coefficient (NSE). The calculation procedure for CC, RMSE, PBIAS, and NSE are given in Eqs. (3)–(6), respectively. The O_i represents the observed variable and P_i is the simulated variable at a time step i. The $\bar{P}$ and $\bar{O}$ denote the average simulated and observed values of the same variable, respectively

$$\text{CC} = \frac{[\sum_{i=1}^n (P_i - \bar{P})(O_i - \bar{O})]^2}{\sum_{i=1}^n (P_i - \bar{P})^2 \sum_{i=1}^n (O_i - \bar{O})^2} \tag{3}$$

$$\text{RMSE} = \sqrt[2]{\frac{1}{n}\sum_{i=12}^{n} (P_i - O_i)^2} \tag{4}$$

$$\text{PBIAS} = \frac{\sum_{i=1}^n (P_i - O_i)}{\sum_{i=1}^n O_i} \tag{5}$$

$$\text{NSE} = 1 - \frac{\sum_{i=1}^n (P_i - \bar{P})}{\sum_{i=1}^n (O_i - \bar{O})} \tag{6}$$

Table 2. List of parameters and their default ranges used for the SWAT model development

Type	Parameter	Description	SWAT default range	
			Minimum	Maximum
r__	CN2	SCSII curve number	−0.3	0.3
r__	SOL_AWC	Average available soil water content	−0.3	0.3
r__	ESCO	Soil evaporation compensation factor	−0.4	0.4
v__	EPCO	Plant uptake factor	0.01	1
r__	SURLAG	Surface runoff lag coefficient	−0.2	0.2
v__	CH_N2	Manning's n value for the main channel	0.016	0.033
v__	CH_K2	Effective soil hydraulic conductivity (mm/hr)	5	150
r__	OV_N	Overland flow Manning's coefficient	−0.4	0.4
r__	ALPHA_BF	Base-flow recession factor (days)	−0.3	0.3
v__	GW_REVAP	Groundwater revap coefficient	0.02	0.2
v__	GW_DELAY	Groundwater delay time (days)	0	500
v__	GWQMN	Threshold water depth in shallow aquifer requires for return flow to occur	0	5,000
r__	SOL_K	Saturated hydraulic conductivity (mm/day)	−0.3	0.3
r__	REVAPMN	Threshold water depth in shallow aquifer requires for revap to occur	−0.3	0.3
r__	RCHRG_DP	Deep aquifer percolation fraction	−0.3	0.3
v__	SFTMP	Mean temperature of snowmelt (°C)	−5	5
v__	SMTMP	Snowmelt base temperature (°C)	−5	5
v__	SMFMX	Maximum melt factor (mm H2O/°C-day)	1.7	6.5
v__	SMFMN	Minimum melt factor (mm H2O/°C-day)	1.4	4.5
v__	TIMP	Snow pack temperature lag factor	0.01	1
v__	SNOCOVMX	Minimum snow water content corresponds to 100% snow cover (mm H2O)	0	1
v__	SNO50COV	Fraction of snow volume represented by SNOCOVMX corresponds to 50% snow cover	0.01	0.99

Note: v__ indicates default parameter is replaced by a given value; and r__ indicates the existing parameter value is multiplied by (1 + the given value).

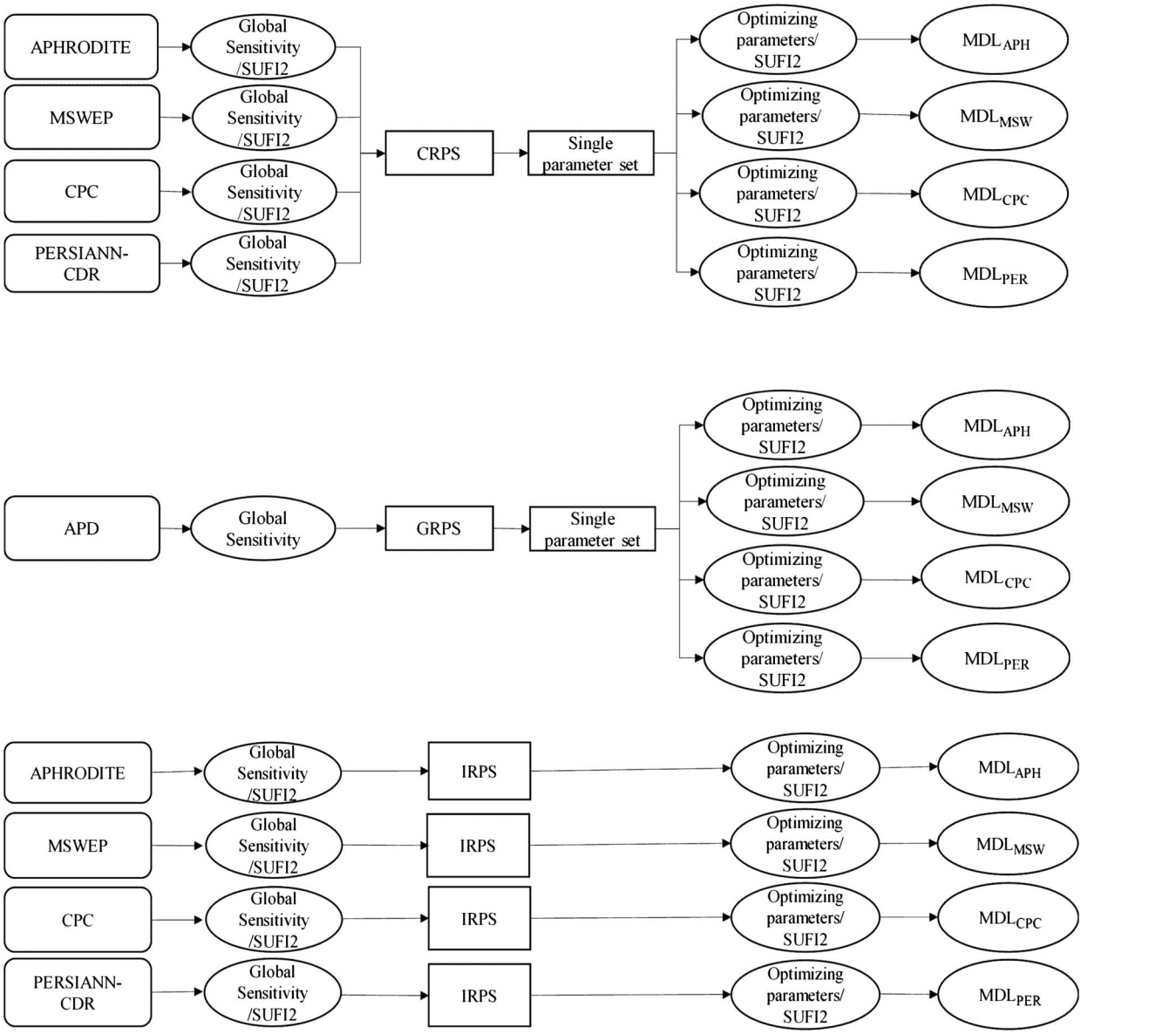

Fig. 2. Flow chart of three calibration procedures (CRPS, GRPS, and IRPS from top to bottom) used in SWAT model ran with four PDS and APD data sets.

Table 3. Ranks of the most sensitive model parameters resulted from sensitivity analysis for all PDSs used in the CRPS approach

Parameter	MDL_{APH}	MDL_{MSW}	MDL_{CPC}	MDL_{PER}	Average
SOL_AWC	2	1	4	2	2.75
CH_K2	1	2	14	1	4.75
SFTMP	3	5	2	4	8
OV_N	11	13	1	8	9.75
CN2	4	22	7	5	12
GW_REVAP	6	8	5	10	12.25
EPCO	22	3	19	3	12.5
ALPHA_BF	10	11	16	14	16.5

Results

Comparison between PDS and APD Data

The spatiotemporal variation of long-term precipitation climatology from the four PDSs (APHRODITE, MSWEP, CPC, and PERSIANN-CDR) is compared with the actual precipitation represented by APD data. As described earlier, all PDSs are available for the period (1979–1997), except PERSIANN-CDR data for the period (1983–1997), while the APD precipitation data set is available for the period 1953–1963. Because PDS and APD data are available in different time periods, we performed the following statistical analysis to compare between these data sets.

First, we plotted the autocorrelation plot to investigate the degree of similarity between APD and PDS time series and a lagged version of itself over successive time intervals. Using autocorrelation plot it is possible to investigate temporal patterns, such as the presence of a periodic signals. Fig. 3 provides the autocorrelation plot for monthly precipitation data of APD and PDS time series at the Mosul station. Note that both APD and all PDS (except CPC data) time series witness similar temporal pattern in terms of magnitude of seasonal fluctuations in correlation coefficient. Based on this preliminary analysis, it is expected that CPC data may not be a good choice for streamflow simulation.

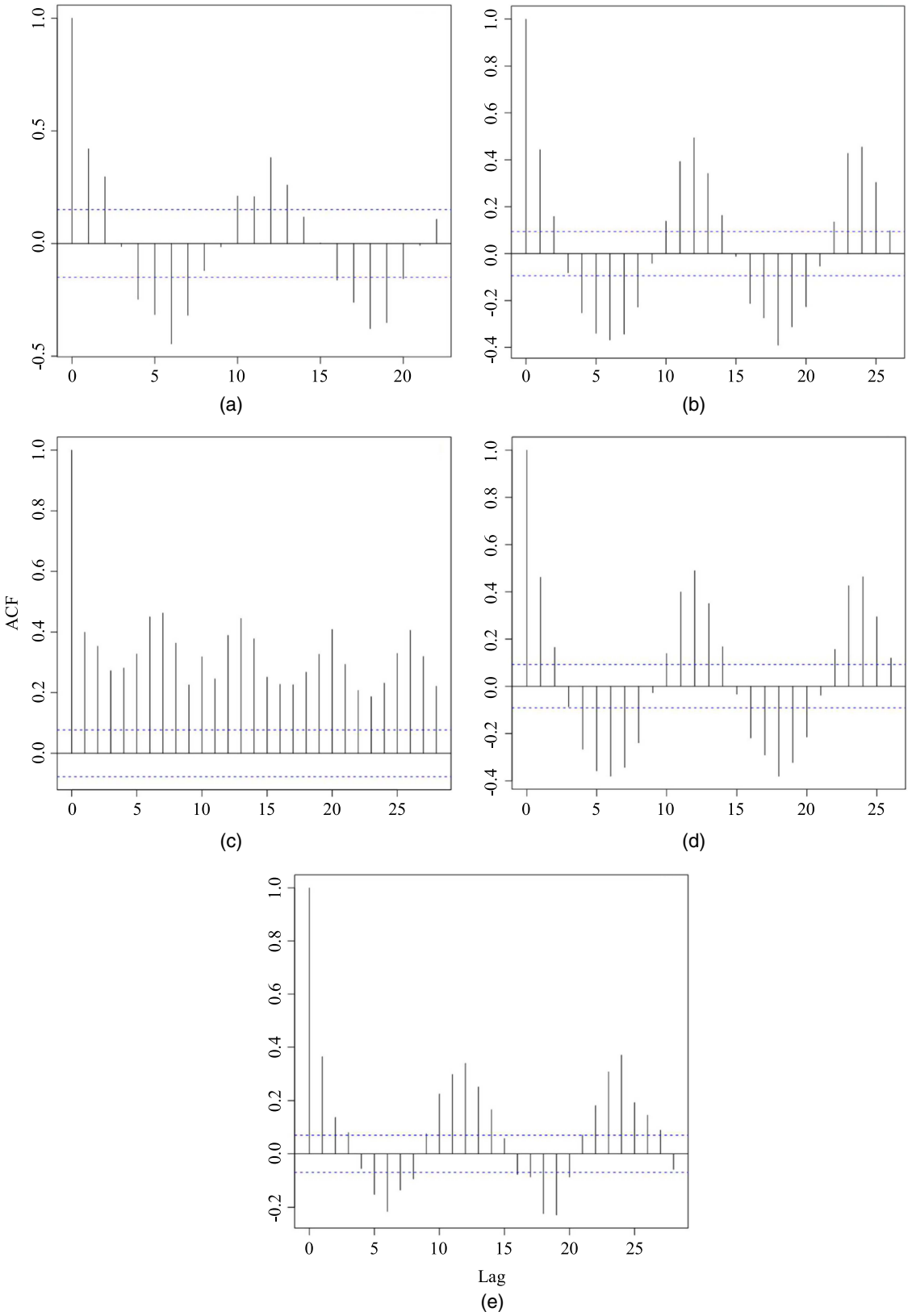

Fig. 3. Autocorrelation function (ACF) plots based on the monthly precipitation from APD and PDS's at Mosul gauge station: (a) APD; (b) APHRODITE; (c) CPC; (d) MSWEP; and (e) PERSIANN-CDR.

Fig. 4 illustrates the spatial distribution of the cross correlation (zero-lag) between APD and PDS over the TRB. Because the APD and PDS data sets are available in different time periods, we used long-term monthly means (monthly climatology) for each data set to estimate the cross correlation between the PDS and the APD. The values shown in Fig. 4 represent the coefficient of correlation that typically varies from -1 to $+1$. It can be observed that the correlation pattern between APD and PDS varies based on the type

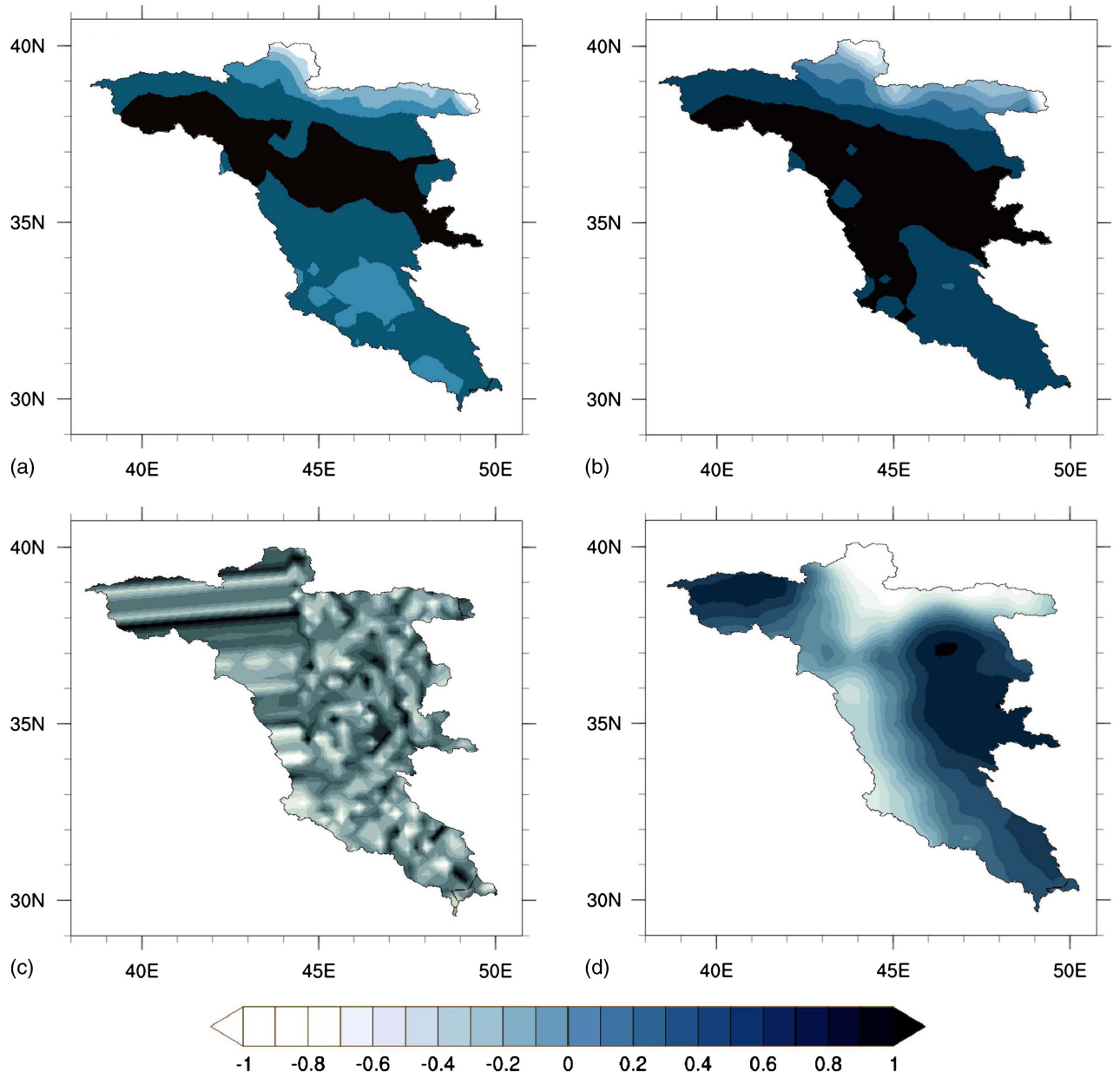

Fig. 4. Cross correlation map (at zero-lag) between long-term mean monthly precipitation climatology from APD and PDSs over the TRB: (a) APHRODITE; (b) MSWEP; (c) CPC; and (d) PERSIANN-CDR.

of the climate; for example, higher cross correlation observed for regions with higher precipitation, and lower correlation at regions with relatively less precipitation. The correlation strength between APD, APRODITE, and MSWEP is comparatively stronger in comparison to CPC and PERSIANN-CDR over the entire river basin. APHRODITE and MSWEP have similar spatial correlation structure compared to APD, whereas CPC and PERSIANN-CDR performed differentially. For example, PERISAN-CDR comparatively performed well in regions with moderate precipitation (e.g., northwest and southeast); conversely, CPC data performed poorly over the TRB with no clear pattern in annual cross correlation. Based on this similarity (dissimilarity) in spatial correlation analysis, it is expected that the performance of PDS likely to differ for streamflow simulation. It is worth investigating and identifying the best PDS that can be used to generate reliable streamflow for different water resource applications.

The correlation strength between APD and PDS was evaluated at selected precipitation gauge stations located in different parts of the TRB. The selected locations are Baghdad, Mosul, Nasiriya, Diala, Hawija, and Hindiya, which are located at 33.33°N, 44.40°E; 36.31°N, 43.15°E; 31.01°N, 46.23°E; 34.08°N, 45.01°E; 33.51°N, 44.30°E; and 32.70°N, 44.28°E, respectively. First, the PDS data are interpolated at these gauge locations, then the long-term mean monthly precipitation is estimated to find the coefficient of determination between them at the selected locations. The values of coefficient of determination (R^2) between APD and PDS based on individual months are shown in Fig. 5. Overall, a positive correlation was observed between APD and PDS, and the stronger correlation strength was observed with respect to APHRODITE and MSWEP data sets for most of the months. However, the performance of CPC data is comparatively poor with respect to other PDS data sets. This figure demonstrates the consistency between the

APHRODITE and MSWEP data sets with the actual precipitation data used for validating other precipitation products.

In order to capture the rainy days signals between APD and PDS, we calculated the average number of rainy days for individual months (Fig. 6). Considering the TRB is mostly located in a semi-arid climate, we selected 0.3 mm as a threshold value to define a rainy day (Awulachew et al. 2007). In general, it was observed that the rainy days signals from APRODITE, and MSWEP showed similarities with APD. It is expected that the distribution of rainy days likely to be different due to the potential impact of global warming and climate change during recent decades for PDS compared to APD data. The CPC performed poorly to capture the rainy days signals especially during dry months. In contrast, the number of rainy days captured by PERSIANN-CDR is reasonably observed at some gauge stations such as Hawija and Hindia.

Considering that the APD and PDS data are available in different time periods, it is a major limitation to compare their correlation results between precipitation and runoff. Therefore, to demonstrate the correlation strength between precipitation and streamflow, we plotted the scattered plot for these two variables at a monthly timescale (Fig. 7). A positive correlation was observed between streamflow and precipitation at selected streamflow gauge stations. Higher correlation was observed for wet spells, and comparatively low correlation observed for dry spells. However, note that the

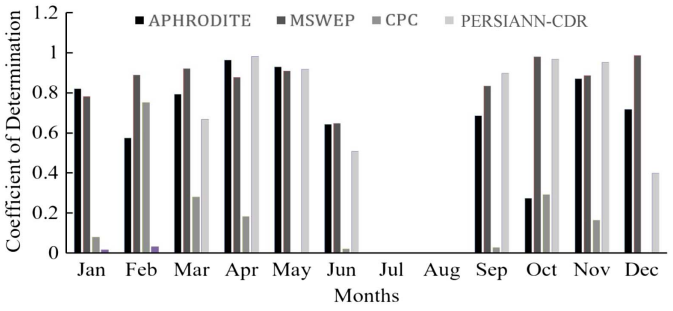

Fig. 5. Coefficient of determination plot based on long-term monthly precipitation from APD and PDSs evaluated at a sample of gauge stations: Baghdad, Mosul, Nasiriya, and Hindiya.

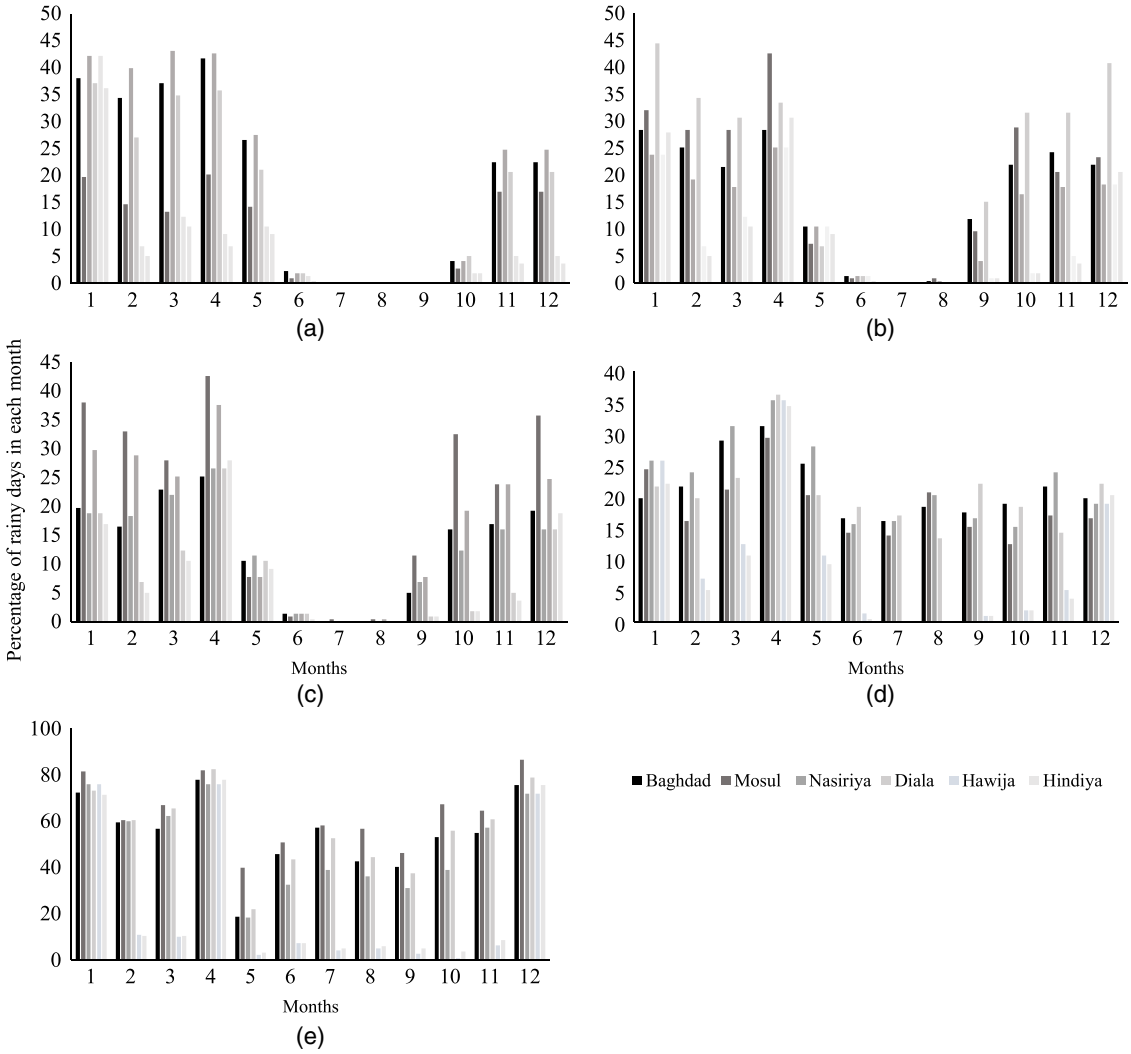

Fig. 6. The percentage of rainy days for individual months between APD and PDSs used in this study: (a) APD; (b) APHRODITE; (c) MSWEP; (d) CPC; and (e) PERSIANN-CDR.

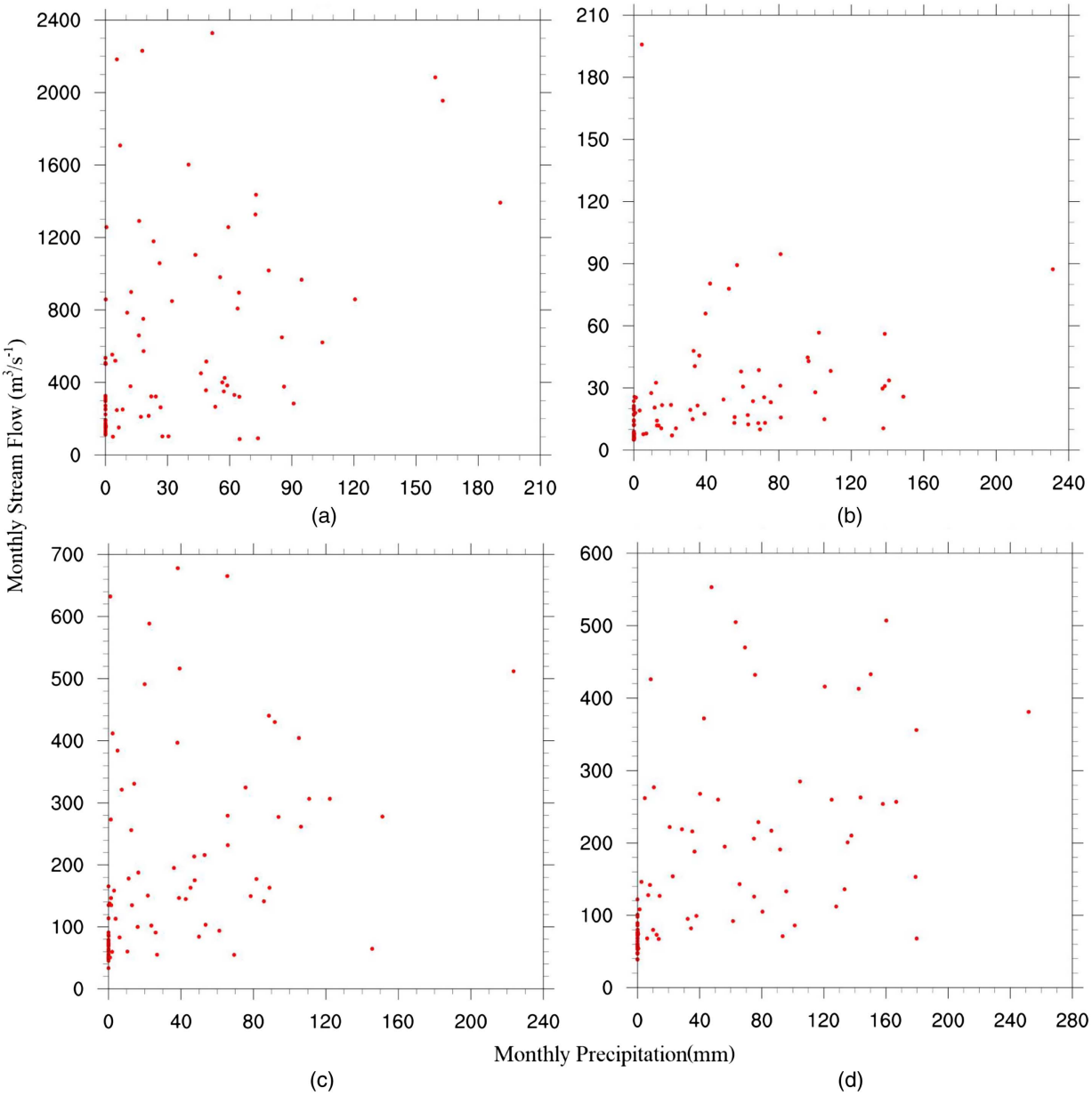

Fig. 7. Scatter plots between monthly precipitation and streamflow at the selected locations: (a) Tigris River at Mosul (TIGBSN1); (b) Khazir River at Manquba (TIGBSN3); (c) Greater Zab River at Eski-Kelek (TIGBSN4); and (d) Diyala River at Derbindi-Khan (TIGBSN8).

correlation strength between precipitation and runoff in a very large river basin located semiarid climate may not be significant as streamflow is controlled by both climate and catchment characteristics. Although, the cross (or lagged) correlation plays a very important role for statistical forecasting models, that completely ignores catchment characteristics. However, in our study we are using a physically-based hydrologic model for streamflow simulation, which considers a combination of climate inputs and catchment characteristics (e.g., land use and soil type).

Uncertainty in SWAT Model Parameters

Five sets of precipitation products APHRODITE (*APH*), MSWEP (*MSW*), CPC, PERSIANN-CDR (*PER*), and actual precipitation data (APD) are used as inputs to SWAT and the corresponding modeled streamflow outputs are represented by MDL_{APH}, MDL_{MSW}, MDL_{CPC}, MDL_{PER}, and MDL_{APD}. The best-fit and the final ranges of the parameters resulted from the calibrated SWAT models for the four PDS (using CRPS) and APD (using GPRS) approaches are compared in Fig. 8. This figure clearly indicates that changing precipitation inputs in the SWAT model produces different sets of parameter uncertainties. Comparing parameter ranges of four models (MDL_{APH}, MDL_{MSW}, MDL_{CPC}, and MDL_{PER}) with MDL_{APD} (the leftmost bars) reveals that parameter range for MDL_{APD} tends to have the least uncertainty (lowest variations). Likewise, MDL_{APH} shows comparatively lower parameter uncertainty compared to the other three models, namely MDL_{MSW}, MDL_{PER}, and MDL_{CPC}. For MDL_{CPC} model, the fitted parameter of SOL_AWC is low, which allows producing more runoff as this precipitation product underestimated the APD data, while the SOL_AWC value in MDL_{MSW} is increased allowing for less runoff as this precipitation overestimated the APD data (Fig. 8).

Most of the rainfall occurs in the northern part of the TRB (where the snowfall is dominant); therefore, the snowmelt temperature

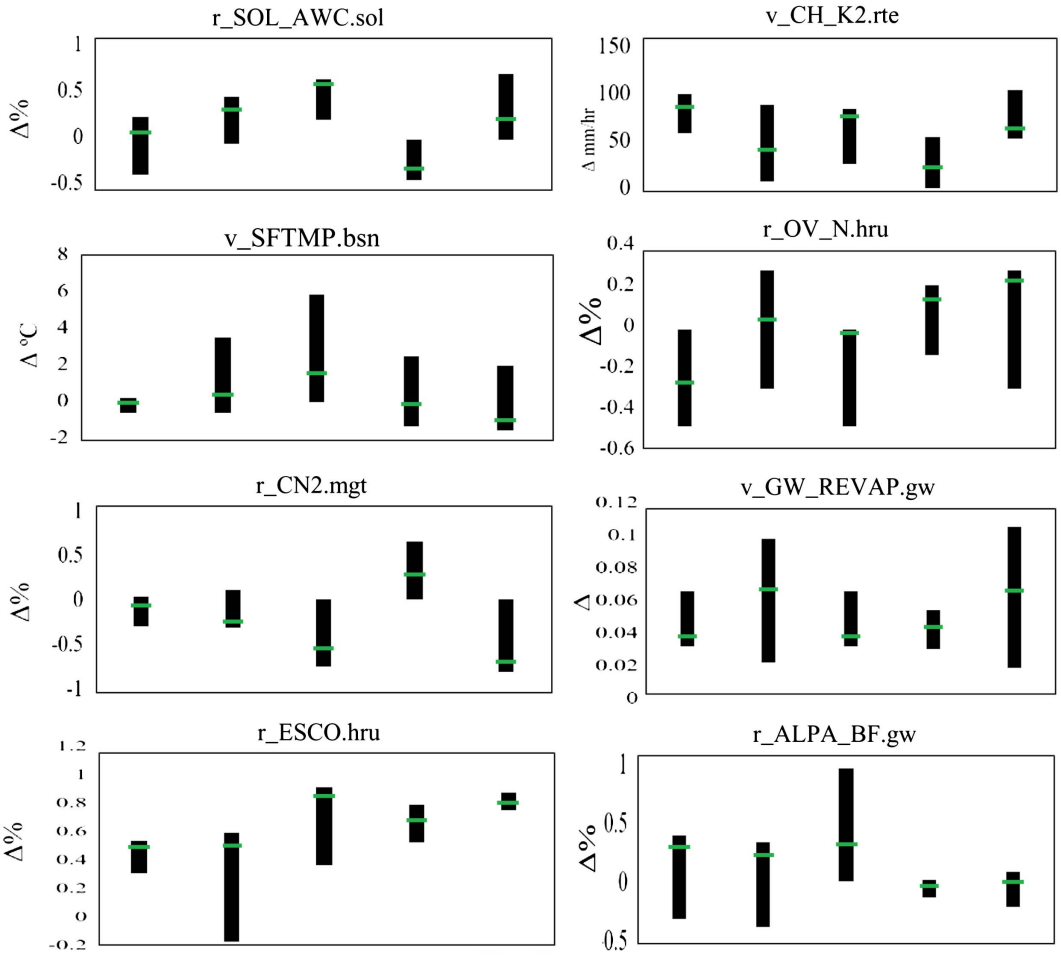

Fig. 8. Ranges of calibrated model parameters and best-fit values (longer horizontal lines) used with SWAT model and derived for five precipitation products.

parameter (SFTMP) seems to be more significant in all models calibrated with PDS. The range of SFTMP value uniformly varies between models with a range of −1°C to 2°C, which is consistent with other studies in similar climate regions, e.g., Iran (Rostamian et al. 2008). The best fit of the hydraulic conductivity for alluvial main channel value (CH_K2) indicates that the main channels in the TRB are covered primarily with clean sand and gravel (CH_K2 > 100 mm/h) to silty sand with gravel (CH_K2 > 50 mm/h). Considering the shallow aquifers in the study area, which primarily consists of sandstone, limestone, and silty soils with a transmissivity ranging from 200 to 560 m^2/day (Jassim and Goff 2006), the CH_K2 values used are reasonable. The shallow aquifer concept in SWAT model refers to the top soil layer that extends to few meters downward, which is in this case automatically defined from soil map by SWAT model.

SWAT classifies precipitation as snow or rain using the average daily temperature, while the snowmelt is controlled by air and snow pack temperature (Neitsch et al. 2011). The mean temperature of snowmelt (°C), temperature (SFTMP), and the snow pack temperature lag factor (TIMP) parameters showed higher sensitivity in the TRB models with PDS products. The time delay between precipitation-surface runoff-streamflow depends on many parameters that were carefully calibrated in the SWAT model. For instance, the surface runoff lag coefficient (SURLAG), overland flow Manning's coefficient (OV_N), and snow pack temperature lag factor (TIMP) control the amount of water that runs off and directed to streams.

Overall, the parameter ranges and best fit values vary by changing the precipitation data source in SWAT model, which may need extra attention when considering only one model input as the issue of parameterization is an important task in hydrological model development. This reinforces the idea of using multiple parameter sets including the one derived from the actual precipitation model to validate the other precipitation models with a large number of simulations (>500 simulations), given that the SUFI-2 parameter range width is highly affected by the number of simulations and consequently the simulated streamflow.

Evaluation of Precipitation Products for Streamflow Simulation

The performance of PDS was evaluated for streamflow simulation in SWAT model calibrated using parameters obtained from CRPS for PDS and from GRPS for ADP. The simulated streamflow with each PDS is compared with the actual observations using quantitative statistics (CC, NSE, and PBIAS), as shown in Table 4. The precipitation product is considered to be performing well if the goodness of fit measures satisfy the following thresholds; CC > 0.65, NSE > 0.50, and |PBIAS| < 25% (Duda et al. 2012; Moriasi et al. 2007). Based on these model performance measures, half of

Table 4. Correlation metrics (CC, NS, and PBIAS) between observed and SWAT based streamflow outputs based on different precipitation data sources

Select stations	MDL_{APD}			MDL_{APH}			MDL_{CPC}			MDL_{MSW}			MDL_{PER}		
	CC	NS	PBIAS	CC	NS	PBIAS	CC	NS	PBIAS	CC	NS	PBIAS	CC	NS	PBIAS
TIGBSN1	**0.73/0.63**	**0.71/0.67**	**−18.87/−16.98**	0.60/0.58	0.65/0.63	11.19/10.85	0.53/0.51	**0.65/0.64**	**11.19/10.74**	0.53/0.51	0.65/0.64	−11.19/−10.74	0.46/0.44	**0.69/0.67**	**11.97/11.49**
TIGBSN2	0.52/0.42	0.61/0.58	3.1/2.79	0.62/0.6	0.62/0.6	−5.47/−5.25	0.51/0.48	0.47/0.45	0.73/0.7	0.62/0.59	0.47/0.45	−55.04/−52.84	0.6/0.57	**0.70/0.67**	**10.43/10.02**
TIGBSN3	**0.68/0.58**	**0.69/0.65**	**−4.17/−3.75**	**0.68/0.65**	**0.69/0.67**	**−4.17/−4.03**	0.57/0.55	0.35/0.33	19.77/19.11	0.53/0.52	0.72/0.7	−23.9/−23.11	0.12/0.11	0.32/0.3	14.87/14.38
TIGBSN4	**0.87/0.77**	**0.98/0.93**	**6.3/5.67**	**0.74/0.72**	**0.72/0.7**	**7.17/6.97**	0.42/0.4	0.24/0.23	23.3/22.65	**0.96/0.94**	**0.99/0.96**	**−9.93/−9.66**	0.61/0.59	**0.91/0.88**	**23.7/23.04**
TIGBSN5	0.52/0.42	0.61/0.58	−2.17/−1.95	0.59/0.54	0.8/0.74	6.37/5.84	0.63/0.57	0.32/0.29	1.27/1.16	0.57/0.52	0.53/0.49	−34.12/−31.29	0.48/0.44	0.43/0.39	−12.5/−11.46
TIGBSN6	0.53/0.43	0.62/0.59	−10.03/−9.03	**0.78/0.74**	**0.98/0.92**	**−7.57/−7.14**	0.43/0.4	0.12/0.11	25.4/23.95	0.53/0.5	0.6/0.57	−10.03/−9.46	0.35/0.33	0.49/0.46	10.93/10.31
TIGBSN7	**0.95/0.85**	**0.86/0.82**	**0.2/0.18**	**0.95/0.88**	**0.86/0.8**	**0.2/0.19**	0.89/0.83	0.26/0.25	3.33/3.1	**0.9/0.83**	**0.82/0.76**	**−0.2/−0.19**	0.47/0.44	**0.74/0.68**	**5.37/4.99**
TIGBSN8	0.5/0.4	0.75/0.72	−26.57/−23.91	0.48/0.44	0.7/0.64	−26.57/−24.44	0.48/0.44	**0.7/0.64**	**26.57/24.44**	0.48/0.44	0.7/0.64	−26.57/−24.44	0.48/0.44	**0.70/0.64**	**−26.57/−24.44**
TIGBSN9	0.42/0.32	0.6/0.57	−20.6/−18.54	0.42/0.39	0.6/0.57	−20.6/−19.36	0.43/0.4	**0.64/0.6**	**20.47/19.24**	0.48/0.45	0.53/0.49	−19.5/−18.33	0.48/0.45	0.53/0.49	−19.5/−18.33
TIGBSN10	**0.62/0.52**	**0.69/0.66**	**−23.9/−21.51**	0.43/0.41	0.63/0.6	−14.84/−14.25	0.43/0.41	**0.62/0.61**	**19.23/18.46**	0.43/0.41	0.38/0.36	−19.26/−18.49	0.17/0.16	**0.66/0.64**	**−24.02/−23.06**

Note: Each cell has two values representing calibration and validation, respectively. Bold values represent significance level of 5%.

the streamflow simulated in MDL_{APD}, driven by actual precipitation data (i.e., APD) satisfied the goodness of fit performance criteria. This seems to emphasize the significance of using point-based precipitation data in representing the spatiotemporal variability even in relatively large-scale watersheds, such as the TRB. Satisfying the goodness of fit criteria by only half of the stations also shows the complexity of the relationship between the daily rainfall and the generated streamflow. For all other precipitation sources (products), the goodness of fit performance indicators are relatively higher during calibration than validation period. The best individual streamflow prediction among all PDS was obtained from MDL_{APH}, which suggests that APHRODITE performed better in hydrological modeling compared to other gauged-based global precipitation products (i.e., CPC and MSWEP), especially in areas that witness high precipitation variability and lack of data (Table 4). The possible reason could be because of the dense gauge representation in case of APHRODITE over the global grid-based precipitation data. In addition, global precipitation data are often available on coarser grid scale, which may misrepresent the spatial variability information in precipitation data.

Among all PDS, MDL_{CPC} performed poorly for most of the streamflow stations during calibration and validation periods, even though it is compiled from an observed data. Part of this poor performance might be the CPC precipitation data is given on coarser mesh grid data points than all other PDS (i.e., 0.5° compared 0.25° longitude × latitude). This is consistent with the precipitation comparison results obtained in the previous section. The poor correlation between simulated and observed precipitation as well as streamflow simulation using CPC brings into question the credibility of this precipitation product in the hydrologic simulation, and indicates that further process might be required to enhance the spatiotemporal representation for the simulated streamflow data (e.g., downscaling). In contrast, PERSIANN-CDR data performed relatively well based on only NSE and PBIAS criteria. Given that PERSIANN-CDR is satellite data and available for areas with limited data measurements, it can be considered invaluable for hydrological modeling in the TRB. These findings are in accordance with the results of Behrangi et al. (2011), Sidike et al. (2016), and Zhu et al. (2016), where PERSIANN-CDR data showed potentially encouraging results in simulating monthly streamflow data when evaluated against actual point-based precipitation data.

The monthly streamflow simulated by all PDS for the period 1983–1997 (consistent for all models) is presented in Figs. 9 and 10. This analysis was carried out based on the SWAT-CUP best fit streamflow outputs at four discharge stations, out of which two stations (TIGBSN1 and TIGBSN7) are located on the main Tigris River and the other two on its tributaries (TIGBSN4 and TIGBSN6). These stations represent different flow conditions and climate zones in the watershed. Note that the flow in these stations is governed by the snowmelt, which is evident from high flows (regular peaks) in spring months (March–May) and low flows in dry months (May–October). Simulated streamflow outputs show that the individual precipitation product has significant variations compared to the actual streamflow, particularly the peak flow in the TRB during this period. Except for MDL_{MSW} (where the peak flow and the base flow are overpredicted), the base flow in all models was mostly overpredicted, while the peak flow was underpredicted during calibration and validation periods as indicated by the time series. However, the performance of all the models was relatively higher in capturing base flow, especially in the calibration period. This is most likely due to two main reasons; most precipitation products have failed to reproduce extreme events with higher accuracy, and the complexity of the branching system of the main Tigris River before the station locations has made the river routing process more difficult.

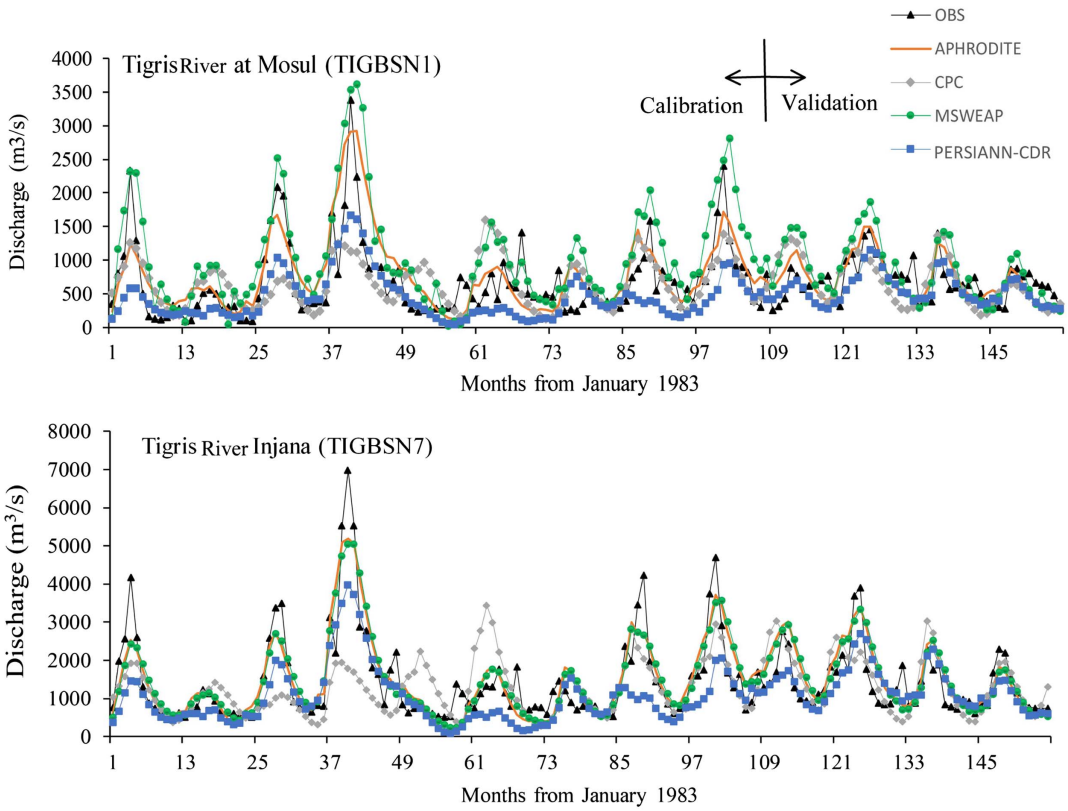

Fig. 9. Simulated monthly streamflow estimated from SWAT model with different PDS for selected locations (TIGBSN1 and TIGBSN7) located on the main Tigris River.

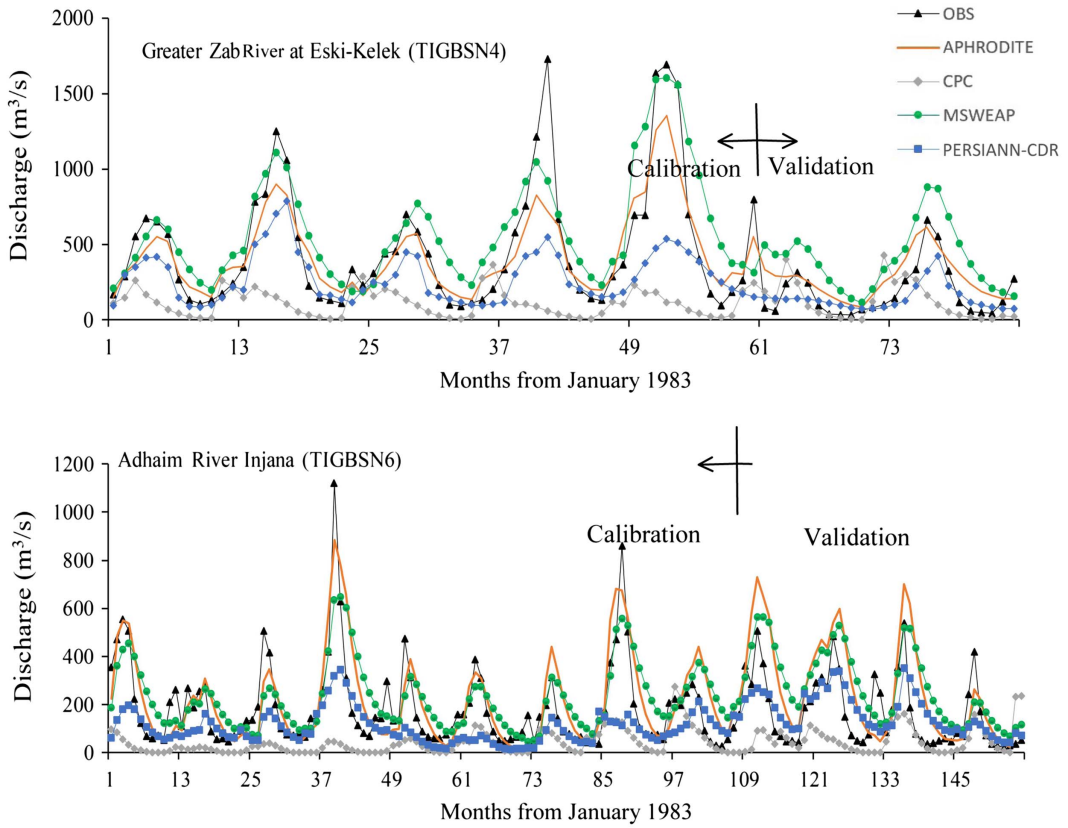

Fig. 10. Simulated monthly streamflow estimated from SWAT model with different PDS for selected locations (TIGBSN4 and TIGBSN6) located on Tigris' river tributaries.

APHRODITE-based streamflow (i.e., MDL_{APH}) in both calibration and validation periods comparatively match well with the observed streamflow, where the model follows similar patterns of the peaks and the low flows for all stations (Figs. 9 and 10).

As stated previously, MDL_{APH} driven by APHRODITE precipitation data source performed relatively better than MDL_{CPC}, MDL_{MSW}, and MDL_{PER} in terms of CC, NSE, and PBIAS during both calibration and validation periods. Even though PERSIANN-CDR precipitation dataset underpredicted the stream flow in the TRB, it performed satisfactorily in matching the actual stream flow at some stations (e.g., TIGBSN1 and TIGBSN7). The CPC precipitation dataset did not perform well as stated previously. These results are consistent with the findings of Vu et al. (2012) and Yang et al. (2015). As expected, the performance of all individual models is slightly higher in calibration than validation period. This is quite likely due to the significant increase in irrigation and drinking water demands in the TRB for later years of simulations (i.e., during validation period) (Issa et al. 2014; Tigrek and Kibaroglu 2011).

Model Streamflow Predictive Uncertainties

Parameter uncertainty in hydrological model is likely to contribute randomness to modeled streamflow outputs (Abbaspour et al. 2015). Predictive uncertainties in modeled streamflow outputs are compared between the four PDS calibrated using the three approaches (CRPS, GRPS, and IRPS). The model is considered to perform well if more than 70% of the observed streamflow was captured during the simulation (i.e., p-factor $> 70\%$) and with smaller 95PPU uncertainty envelope (i.e., r-factor of about 1).

Simulation uncertainty represented by both the p- and r-factors was evaluated for each precipitation product calibrated using CRPS, GRPS, and IRPS approaches and presented in Fig. 11. The values of these two factors are presented by using four groups of box plots. Each group represents a model calibrated using CRPS, GRPS, and IPRS. Three pairs of boxes are presented in each group. For each pair, the first box plot represents calibration and the second box plot is for validation. For all three approaches, p-factor and r-factor values are higher during calibration than validation period. The p- and r-factors from IRPS and GRPS approaches scored higher values than the CRPS. The highest values for p- and r-factors are observed for MDL_{APH} and MDL_{MSW} (with a relative percentage increase of under 8% in both p- and r-factors for GRPS), which means that these two calibration approaches have less predictive uncertainties in simulating streamflow. The relative improvements in SWAT model simulations calibrated with GRPS over IRPS is likely due to the higher/lower curve number values used in SWAT model than the standard tabulated ranges. The higher accuracy in streamflow estimations for the case of GRPS came on the expense of the calibrated parameter ranges. This exercise of not using the standard tabulated parameter values was also mentioned by Bitew et al. (2012), which could cause substantial errors to the simulated streamflow, if it is not closely monitored. All stations based on MDL_{APH} witnessed the lowest uncertainty, while MDL_{CPC} shows the highest predicted uncertainty, which makes this precipitation data sources least desirable for prediction streamflow data in TRB. Some gauge stations based on MDL_{MSW} and MDL_{PER} reached desirable uncertainties in calibration and validation periods.

Finally, a comparison between simulated streamflow using the CRPS and IRPS approaches and the actual streamflow is illustrated in Figs. 12 and 13. The left side panel represents simulation results for CRPS calibration approach, while the right column is simulation results obtained based on IRPS approach. In these two figures,

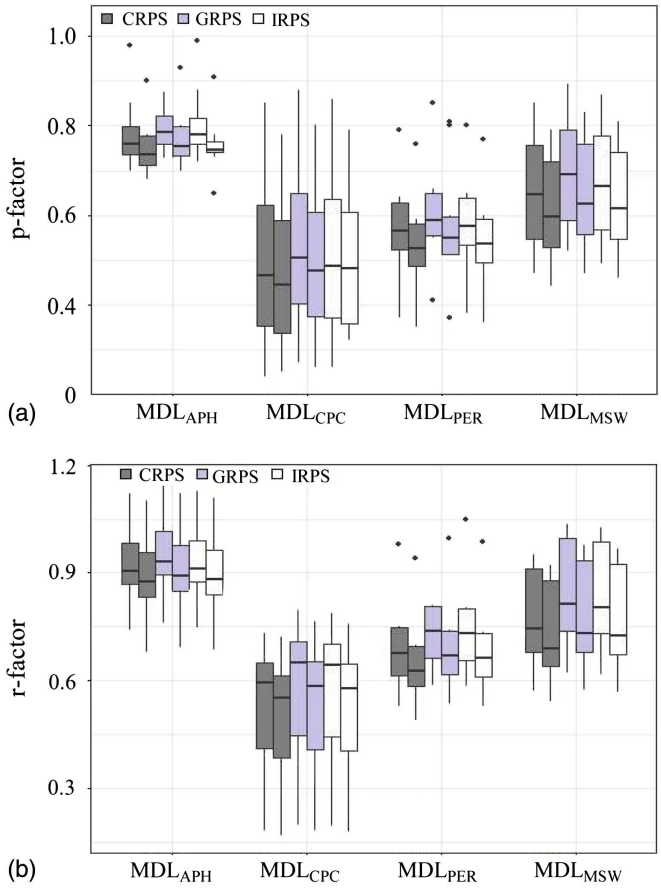

Fig. 11. p- and r-factors from SWAT models (shown as groups) calibrated with CRPS, GRPS, and IRPS methods. Each group represents a model calibrated using three approaches.

predictive uncertainty is represented for a sample of two stations (TIGBSN2 and TIGBSN3) located in the highlands and lowlands of the TRB, respectively. By comparing the 95PPU of models from CRPS and IRPS (left and right panels, respectively), the IRPS shows less predictive uncertainty than the CRPS approach (i.e., better streamflow simulations). In addition, the uncertainty bandwidth was relatively narrower during low flow conditions than high flows. The MDL_{APH} model [Figs. 12(a) and 13(a)] witnessed consistently the lowest uncertainty compared to the other three data sources. The other three modeled streamflow outputs (MDL_{CPC}, MDL_{MSE}, and MDL_{PER}) were unable to capture the extreme streamflow accurately for the entire time series. However, MDL_{PER} showed reduced uncertainty at some stations when the IPRS calibration approach is used [compare Figs. 12(d) and 13(d)]. Overall, PERSIANN-CDR precipitation data can be a possible source for evaluating monthly streamflow in the TRB.

Different precipitation inputs generate distinct prediction uncertainties in modeling streamflow. The results are heterogeneous, and it is not possible to generalize the outcomes obtained in one subcatchment to another, i.e., the prediction uncertainty of each precipitation product is basin-specific. These variations of simulated streamflow uncertainties in response to different input precipitations could be attributed to the different interpolation techniques and merging algorithms that were implemented to compile these precipitation datasets (Tuo et al. 2016). Failing to capture extreme streamflow might be due to the relatively large number of iterations needed by SUFI-2, which is usually used in calibrating models (Strauch et al. 2012).

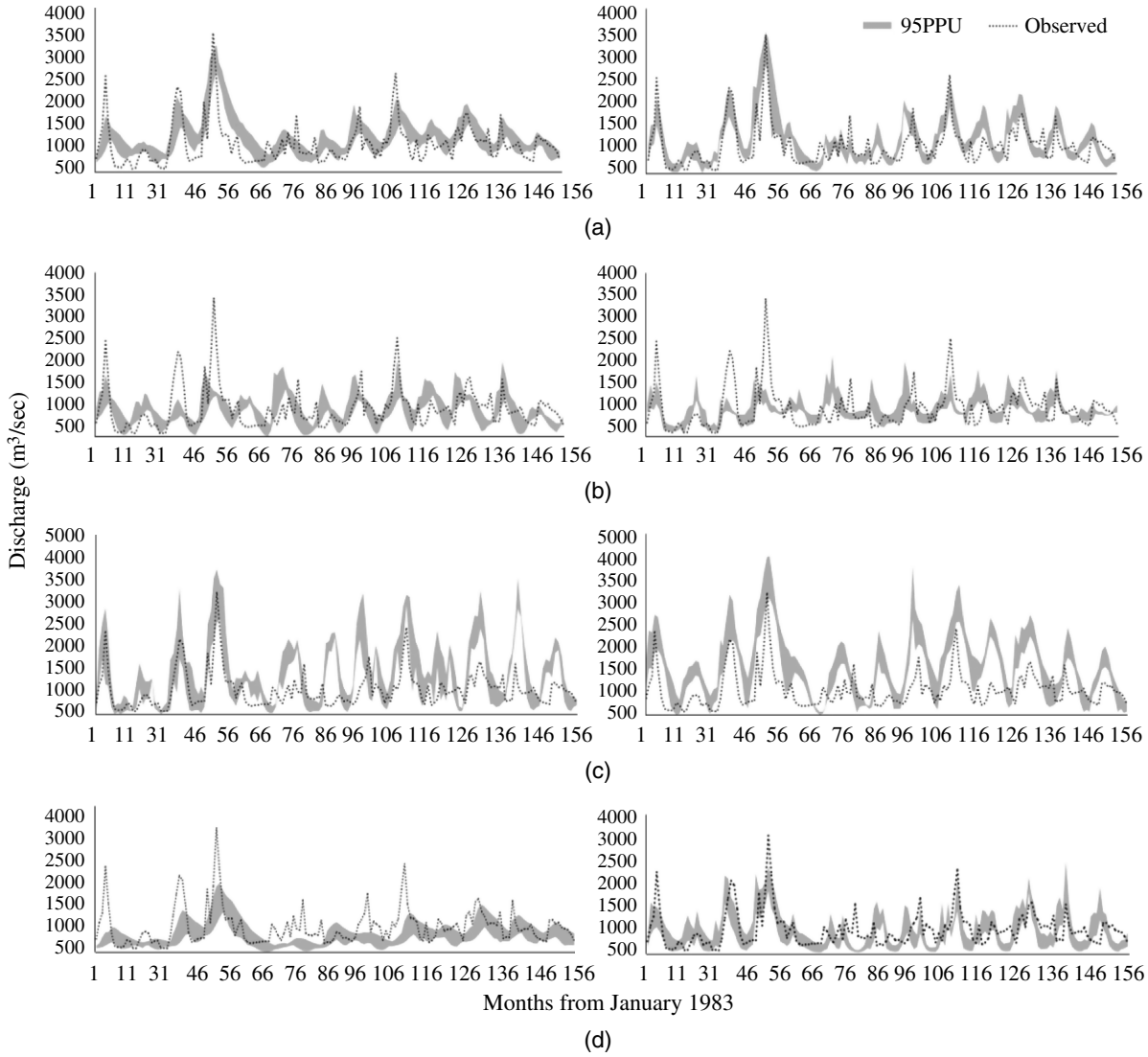

Fig. 12. Illustration of 95PPU intervals obtained from SUFI-2 for CRPS and IRPS approaches. Model results are presented for TIGBSN2 streamflow station. Rows are arranged as follows: (a) APHRODITE; (b) CPC; (c) MSWEP; and (d) PERSIANN-CDR.

Conclusion

This study investigates the spatiotemporal variations of four precipitation data sources and evaluates their performance on simulating streamflow for the Tigris River basin where the ground-based precipitation observations are scarce. Precipitation data sources consist of APHRODITE, CPC, MSWEP, and PERSIANN-CDR. The long-term precipitation estimates from these data sources are compared with the actual gauged precipitation data available for 33 stations for the study area. In addition, the performance of these data source for simulating monthly streamflow was investigate using a hydrologic modeling framework. The following conclusions are drawn from this study:

- All four precipitation data sources have produced different biases when evaluated against actual rain gauges. APHRODITE precipitation data showed the best acceptable spatiotemporal variations over Tigris River basin. Conversely, MSWEP data overestimated the actual gauge precipitation data while CPC underestimated the actual precipitation data. PERSIANN-CDR satellite-based precipitation data showed a satisfactory comparison with observed precipitation data.
- Monthly streamflow estimated by SWAT model significantly improved using observed rainfall information in comparison to selected precipitation data sources because of the biases associated with each data source. Among the precipitation data sources, APHRODITE (interpolated from dense number of gauges per grid) exhibited the best skills in representing the streamflow, while PERSIANN-CDR (satellite data) showed satisfactory performance at few locations in the Tigris River basin. Thus, it can be considered as a favorable product for the Tigris River basin in case of scarce precipitation records.
- Predicted uncertainties in streamflow simulations vary when different parameter sets used in the SWAT model. Therefore, multiple calibration approaches may be utilized to identify better model parameter sets. SWAT model calibrated individually with each precipitation data source showed the best calibration practice because it produced the least predictive uncertainties with realistic parameter range representations.
- The streamflow estimated for the Tigris River basin using different forcing precipitations are heterogeneous and it is not straightforward to generalize the outcomes obtained in one catchment to another, which also means the prediction uncertainty of each

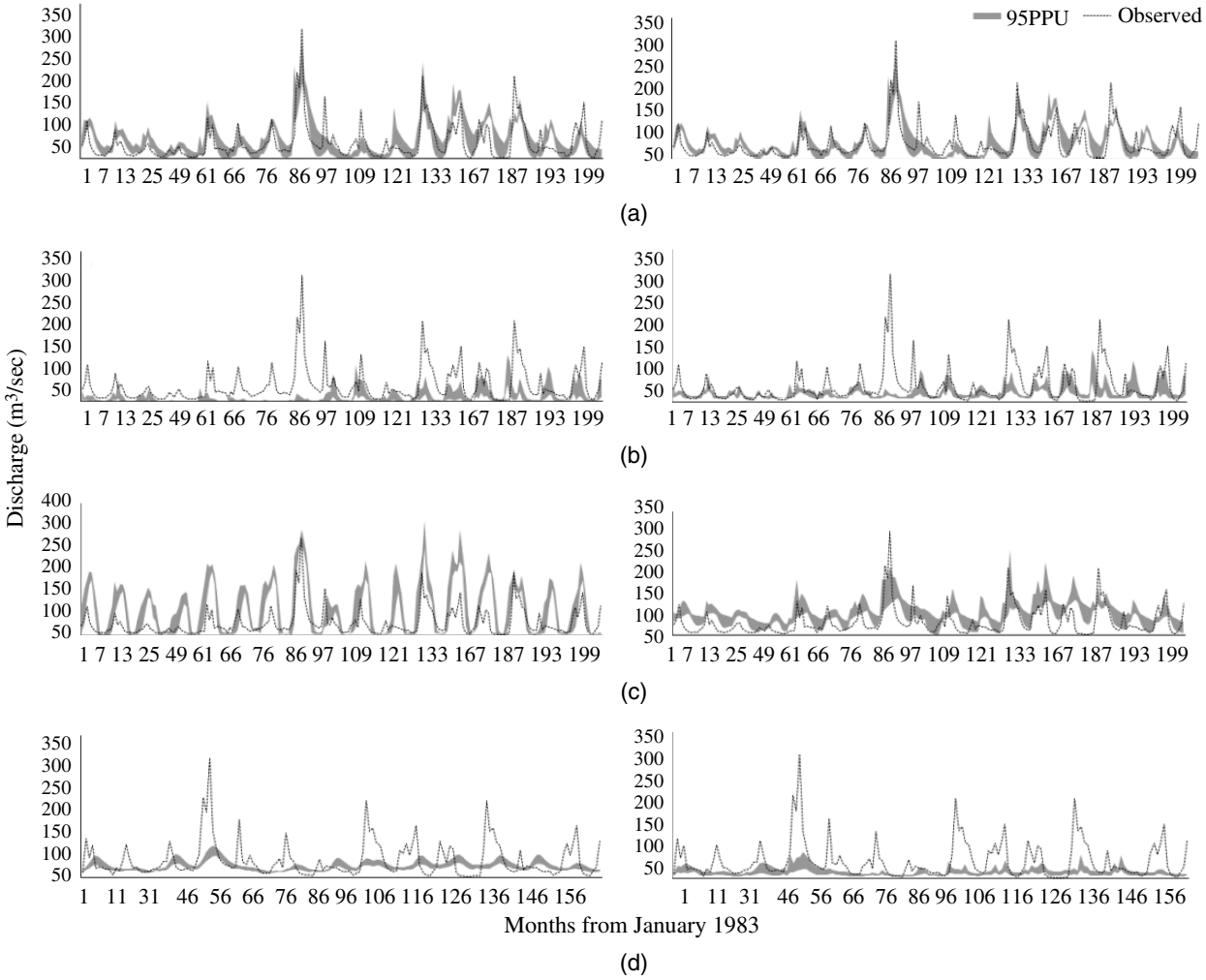

Fig. 13. Illustration of 95PPU intervals obtained from SUFI-2 for CRPS and IRPS approaches. Model results are presented for TIGBSN3 streamflow station. Rows are arranged as follows: (a) APHRODITE; (b) CPC; (c) MSWEP; and (d) PERSIANN-CDR.

precipitation product is basin-specific (i.e., the findings are only applied for the Tigris River basin).

Acknowledgments

The authors would like acknowledge the Higher Committee for Education Development, Iraq, for sponsoring this study. This study was supported by the National Science Foundation (NSF) Award No. 1653841. We would also like to extend our gratitude to the editor and two anonymous reviewers for their valuable comments that helped us to improve the quality of our manuscript.

References

Abbaspour, K. C., C. A. Johnson, and M. T. Van Genuchten. 2004. "Estimating uncertain flow and transport parameters using a sequential uncertainty fitting procedure." *Vadose Zone J.* 3 (4): 1340–1352. https://doi.org/10.2136/vzj2004.1340.

Abbaspour, K. C., E. Rouholahnejad, S. Vaghefi, R. Srinivasan, H. Yang, and B. Kløve. 2015. "A continental-scale hydrology and water quality model for Europe: Calibration and uncertainty of a high-resolution large-scale SWAT model." *J. Hydrol.* 524: 733–752. https://doi.org/10.1016/j.jhydrol.2015.03.027.

Abbaspour, K. C., M. T. Van Genuchten, R. Schulin, and E. Schläppi. 1997. "A sequential uncertainty domain inverse procedure for estimating subsurface flow and transport parameters." *Water Resour. Res.* 33 (8): 1879–1892. https://doi.org/10.1029/97WR01230.

Abbaspour, K. C., J. Yang, I. Maximov, R. Siber, K. Bogner, J. Mieleitner, J. Zobrist, and R. Srinivasan. 2007. "Modelling hydrology and water quality in the pre-alpine/alpine Thur watershed using SWAT." *J. Hydrol.* 333 (2): 413–430. https://doi.org/10.1016/j.jhydrol.2006.09.014.

Ajaaj, A. A., A. K. Mishra, and A. A. Khan. 2016. "Comparison of bias correction techniques for GPCC rainfall data in semi-arid climate." *Stochastic Environ. Res. Risk Assess.* 30 (6): 1659–1675. https://doi.org/10.1007/s00477-015-1155-9.

Amisigo, B., N. Van de Giesen, C. Rogers, W. Andah, and J. Friesen. 2008. "Monthly streamflow prediction in the Volta basin of west Africa: A SISO NARMAX polynomial modelling." *Phys. Chem. Earth Part A/B/C* 33 (1): 141–150. https://doi.org/10.1016/j.pce.2007.04.019.

Andréassian, V., N. Le Moine, C. Perrin, M. H. Ramos, L. Oudin, T. Mathevet, J. Lerat, and L. Berthet. 2012. "All that glitters is not gold: The case of calibrating hydrological models." *Hydrol. Processes* 26 (14): 2206–2210.

Arnold, J., J. Kiniry, R. Srinivasan, J. Williams, E. Haney, and S. Neitsch. 2013. *SWAT 2012 input/output documentation*. College Station, TX: Texas Water Resources Institute.

Arnold, J. G., et al. 2012. "SWAT: Model use, calibration, and validation." *Trans. ASABE* 55 (4): 1491–1508. https://doi.org/10.13031/2013.42256.

Arnold, J. G., and N. Fohrer. 2005. "SWAT2000: Current capabilities and research opportunities in applied watershed modelling." *Hydrol. Processes* 19 (3): 563–572. https://doi.org/10.1002/hyp.5611.

Arnold, J. G., R. Srinivasan, R. S. Muttiah, and J. R. Williams. 1998. "Large area hydrologic modeling and assessment. Part I: Model development." *J. Am. Water Resour. Assoc.* 34 (1): 73–89. https://doi.org/10.1111/j.1752-1688.1998.tb05961.x.

Ashouri, H., K. L. Hsu, S. Sorooshian, D. K. Braithwaite, K. R. Knapp, L. D. Cecil, B. R. Nelson, and O. P. Prat. 2015. "PERSIANN-CDR: Daily precipitation climate data record from multisatellite observations for hydrological and climate studies." *Bull. Am. Meteorol. Soc.* 96 (1): 69–83. https://doi.org/10.1175/BAMS-D-13-00068.1.

Awulachew, S. B., A. D. Yilma, M. Loulseged, W. Loiskandl, M. Ayana, and T. Alamirew. 2007. *Water resources and irrigation development in Ethiopia*. Colombo, Sri Lanka: International Water Management Institute.

Bates, B. C., and E. P. Campbell. 2001. "A Markov chain Monte Carlo scheme for parameter estimation and inference in conceptual rainfall-runoff modeling." *Water Resour. Res.* 37 (4): 937–947. https://doi.org/10.1029/2000WR900363.

Beck, H. E., A. I. van Dijk, V. Levizzani, J. Schellekens, D. G. Miralles, B. Martens, and A. de Roo. 2017. "MSWEP: 3-hourly 0.25 global gridded precipitation (1979–2015) by merging gauge, satellite, and reanalysis data." *Hydrol. Earth Syst. Sci.* 21 (1): 589. https://doi.org/10.5194/hess-21-589-2017.

Behrangi, A., K. Andreadis, J. B. Fisher, F. J. Turk, S. Granger, T. Painter, and N. Das. 2014. "Satellite-based precipitation estimation and its application for streamflow prediction over mountainous western US basins." *J. Appl. Meteorol. Climatol.* 53 (12): 2823–2842. https://doi.org/10.1175/JAMC-D-14-0056.1.

Behrangi, A., B. Khakbaz, T. C. Jaw, A. AghaKouchak, K. Hsu, and S. Sorooshian. 2011. "Hydrologic evaluation of satellite precipitation products over a mid-size basin." *J. Hydrol.* 397 (3): 225–237. https://doi.org/10.1016/j.jhydrol.2010.11.043.

Beven, K. J. 2011. *Rainfall-runoff modelling: The primer*. Lancaster, UK: Wiley.

Bitew, M. M., M. Gebremichael, L. T. Ghebremichael, and Y. A. Bayissa. 2012. "Evaluation of high-resolution satellite rainfall products through streamflow simulation in a hydrological modeling of a small mountainous watershed in Ethiopia." *J. Hydrometeorol.* 13 (1): 338–350. https://doi.org/10.1175/2011JHM1292.1.

Blasone, R.-S., J. A. Vrugt, H. Madsen, D. Rosbjerg, B. A. Robinson, and G. A. Zyvoloski. 2008. "Generalized likelihood uncertainty estimation (GLUE) using adaptive Markov chain Monte Carlo sampling." *Adv. Water Resour.* 31 (4): 630–648. https://doi.org/10.1016/j.advwatres.2007.12.003.

Bozkurt, D., and O. L. Sen. 2011. "Precipitation in the Anatolian peninsula: Sensitivity to increased SSTs in the surrounding seas." *Clim. Dyn.* 36 (3–4): 711–726. https://doi.org/10.1007/s00382-009-0651-3.

Dile, Y. T., and R. Srinivasan. 2014. "Evaluation of CFSR climate data for hydrologic prediction in data-scarce watersheds: An application in the Blue Nile river basin." *J. Am. Water Resour. Assoc.* 50 (5): 1226–1241. https://doi.org/10.1111/jawr.12182.

Duda, R. O., P. E. Hart, and D. G. Stork. 2012. *Pattern classification*. New York: Wiley.

Earls, J., and B. Dixon. 2008. "A comparison of SWAT model-predicted potential evapotranspiration using real and modeled meteorological data." *Vadose Zone J.* 7 (2): 570–580. https://doi.org/10.2136/vzj2007.0012.

FAO (Food and Agriculture Organization of the United Nations). 2013. *The FAO-UNESCO soil map of the world*. Rome: FAO.

Faramarzi, M., K. C. Abbaspour, R. Schulin, and H. Yang. 2009. "Modelling blue and green water resources availability in Iran." *Hydrol. Processes* 23 (3): 486–501. https://doi.org/10.1002/hyp.7160.

Faurès, J. M., D. Goodrich, D. A. Woolhiser, and S. Sorooshian. 1995. "Impact of small-scale spatial rainfall variability on runoff modeling." *J. Hydrol.* 173 (1–4): 309–326. https://doi.org/10.1016/0022-1694(95)02704-S.

Franz, K. J., P. Butcher, and N. K. Ajami. 2010. "Addressing snow model uncertainty for hydrologic prediction." *Adv. Water Resour.* 33 (8): 820–832. https://doi.org/10.1016/j.advwatres.2010.05.004.

Frenken, K. 2009. *Irrigation in the middle east region in figures AQUASTAT survey-2008*. Rome: Food Agriculture Organization.

Fuka, D. R., M. T. Walter, C. MacAlister, A. T. Degaetano, T. S. Steenhuis, and Z. M. Easton. 2014. "Using the climate forecast system reanalysis as weather input data for watershed models." *Hydrol. Processes* 28 (22): 5613–5623. https://doi.org/10.1002/hyp.10073.

Gallagher, M. R., and J. Doherty. 2007. "Parameter interdependence and uncertainty induced by lumping in a hydrologic model." *Water Resour. Res.* 43 (5): 1–18. https://doi.org/10.1029/2006WR005347.

Gassman, P. W., M. R. Reyes, C. H. Green, and J. G. Arnold. 2007. "The soil and water assessment tool: Historical development, applications, and future research directions." *Trans. ASABE* 50 (4): 1211–1250. https://doi.org/10.13031/2013.23637.

Issa, I. E., N. Al-Ansari, G. Sherwany, and S. Knutsson. 2014. "Expected future of water resources within Tigris–Euphrates rivers basin, Iraq." *J. Water Resour. Prot.* 6 (5): 421–432. https://doi.org/10.4236/jwarp.2014.65042.

Jassim, S. Z., and J. C. Goff. 2006. *Geology of Iraq*. London: Geological Society of London.

Jiang, S., L. Ren, Y. Hong, X. Yang, M. Ma, Y. Zhang, and F. Yuan. 2014. "Improvement of multi-satellite real-time precipitation products for ensemble streamflow simulation in a middle latitude basin in south China." *Water Resour. Manage.* 28 (8): 2259–2278. https://doi.org/10.1007/s11269-014-0612-4.

Jiang, S., L. Ren, Y. Hong, B. Yong, X. Yang, F. Yuan, and M. Ma. 2012. "Comprehensive evaluation of multi-satellite precipitation products with a dense rain gauge network and optimally merging their simulated hydrological flows using the Bayesian model averaging method." *J. Hydrol.* 452–453: 213–225. https://doi.org/10.1016/j.jhydrol.2012.05.055.

Jones, C., M. Sultan, E. Yan, A. Milewski, M. Hussein, A. Al-Dousari, S. Al-Kaisy, and R. Becker. 2008. "Hydrologic impacts of engineering projects on the Tigris–Euphrates system and its marshlands." *J. Hydrol.* 353 (1): 59–75. https://doi.org/10.1016/j.jhydrol.2008.01.029.

Karakoc, U., and S. Patil. 2016. "Comparison of TRMM satellite and ground-based precipitation data for predicting streamflow in Kucuk Menderes river basin, Turkey." In Vol. 18 of *EGU General Assembly Conf. Abstracts*. Vienna Austria: EGU General Assembly.

Kibaroğlu, A. 2002. *Building a regime for the waters of the Euphrates–Tigris river basin*. Leiden, Netherlands: Martinus Nijhoff Publishers.

Knapp, K. R. 2008. "Scientific data stewardship of international satellite cloud climatology project B1 global geostationary observations." *J. Appl. Remote Sens.* 2 (1): 023548. https://doi.org/10.1117/1.3043461.

Lee, H., Y. Zhang, D. Seo, and P. Xie. 2015. "Utilizing satellite precipitation estimates for streamflow forecasting via adjustment of mean field bias in precipitation data and assimilation of streamflow observations." *J. Hydrol.* 529 (3): 779–794. https://doi.org/10.1016/j.jhydrol.2015.08.057.

Li, H., Y. Zhang, F. H. Chiew, and S. Xu. 2009. "Predicting runoff in ungauged catchments by using Xinanjiang model with MODIS leaf area index." *J. Hydrol.* 370 (1): 155–162. https://doi.org/10.1016/j.jhydrol.2009.03.003.

Ly, S., C. Charles, and A. Degré. 2013. "Different methods for spatial interpolation of rainfall data for operational hydrology and hydrological modeling at watershed scale: A review." *Biotechnologie, Agronomie, Société et Environnement* 17 (2): 392.

Marghany, M., H. A. Hasab, S. Mansor, and A. R. B. M. Shariff. 2016. "Developing hydrological model for water quality in Iraq marshes zone using Landsat-TM." In *IOP Conf. Series: Earth and Environmental Science*, 012073. Bristol, UK: IOP Publishing.

Miao, C., H. Ashouri, K. L. Hsu, S. Sorooshian, and Q. Duan. 2015. "Evaluation of the PERSIANN-CDR daily rainfall estimates in capturing the behavior of extreme precipitation events over China." *J. Hydrometeorol.* 16 (3): 1387–1396. https://doi.org/10.1175/JHM-D-14-0174.1.

Mishra, A. K., and V. P. Singh. 2010. "Changes in extreme precipitation in Texas." *J. Geophys. Res. Atmos.* 115 (D14): 228–237. https://doi.org/10.1029/2009JD013398.

Moriasi, D. N., J. G. Arnold, M. W. Van Liew, R. L. Bingner, R. D. Harmel, and T. L. Veith. 2007. "Model evaluation guidelines for systematic quantification of accuracy in watershed simulations." *Trans. ASABE* 50 (3): 885–900. https://doi.org/10.13031/2013.23153.

Neitsch, S. L., J. G. Arnold, J. R. Kiniry, and J. R. Williams. 2011. *Soil and water assessment tool theoretical documentation version 2009*. College Station, TX: Texas Water Resources Institute.

Rohstoffe, B. 2013. *Inventory of shared water resources in western Asia*. Beirut, Lebanon: UN-ESCWA.

Rostamian, R., A. Jaleh, M. Afyuni, S. F. Mousavi, M. Heidarpour, A. Jalalian, and K. C. Abbaspour. 2008. "Application of a SWAT model for estimating runoff and sediment in two mountainous basins in central Iran." *Hydrol. Sci. J.* 53 (5): 977–988. https://doi.org/10.1623/hysj.53.5.977.

Saleh, D. K. 2010. "Stream gage descriptions and streamflow statistics for sites in the Tigris river and Euphrates river basins, Iraq." Reston, VA: USGS.

Schuol, J., and K. Abbaspour. 2006. "Calibration and uncertainty issues of a hydrological model (SWAT) applied to west Africa." *Adv. Geosci.* 9 (9): 137–143. https://doi.org/10.5194/adgeo-9-137-2006.

Shahin, M. 2007. *Water resources and hydrometeorology of the Arab region*. Berlin: Springer Science & Business Media.

Sidike, A., X. Chen, T. Liu, K. Durdiev, and Y. Huang. 2016. "Investigating alternative climate data sources for hydrological simulations in the upstream of the Amu Darya river." *Water* 8 (10): 441. https://doi.org/10.3390/w8100441.

Sorooshian, S., K.-L. Hsu, X. Gao, H. V. Gupta, B. Imam, and D. Braithwaite. 2000. "Evaluation of PERSIANN system satellite-based estimates of tropical rainfall." *Bull. Am. Meteorol. Soc.* 81 (9): 2035–2046. https://doi.org/10.1175/1520-0477(2000)081%3C2035:EOPSSE%3E2.3.CO;2.

Strauch, M., C. Bernhofer, S. Koide, M. Volk, C. Lorz, and F. Makeschin. 2012. "Using precipitation data ensemble for uncertainty analysis in SWAT streamflow simulation." *J. Hydrol.* 414: 413–424. https://doi.org/10.1016/j.jhydrol.2011.11.014.

Taesombat, W., and N. Sriwongsitanon. 2009. "Areal rainfall estimation using spatial interpolation techniques." *Sci. Asia* 35 (3): 268–275. https://doi.org/10.2306/scienceasia1513-1874.2009.35.268.

Tateishi, R., et al. 2011. "Production of global land cover data–GLCNMO." *Int. J. Digital Earth* 4 (1): 22–49. https://doi.org/10.1080/17538941003777521.

Thiemig, V., R. Rojas, M. Zambrano-Bigiarini, and A. De Roo. 2013. "Hydrological evaluation of satellite-based rainfall estimates over the Volta and Baro-Akobo basin." *J. Hydrol.* 499: 324–338. https://doi.org/10.1016/j.jhydrol.2013.07.012.

Tigrek, S., and A. Kibaroglu. 2011. "Strategic role of water resources for Turkey." *Turkey's Water Policy*, 27–42. Berlin: Springer.

Tobin, K., and M. Bennett. 2009. "Using SWAT to model streamflow in two river basins with ground and satellite precipitation data." *J. Am. Water Resour. Assoc.* 45 (1): 253–271. https://doi.org/10.1111/j.1752-1688.2008.00276.x.

Tobin, K., and M. Bennett. 2011. "Analysis of adjustment of satellite precipitation for streamflow simulations." *WIT Trans. Ecol. Environ.* 146 (2): 155–166.

Tuo, Y., Z. Duan, M. Disse, and G. Chiogna. 2016. "Evaluation of precipitation input for SWAT modeling in alpine catchment: A case study in the Adige river basin (Italy)." *Sci. Total Environ.* 573 (7): 66–82. https://doi.org/10.1016/j.scitotenv.2016.08.034.

Van Griensven, A., T. Meixner, S. Grunwald, T. Bishop, M. Diluzio, and R. Srinivasan. 2006. "A global sensitivity analysis tool for the parameters of multi-variable catchment models." *J. Hydrol.* 324 (1): 10–23. https://doi.org/10.1016/j.jhydrol.2005.09.008.

Voss, K. A., J. S. Famiglietti, M. Lo, C. Linage, M. Rodell, and S. C. Swenson. 2013. "Groundwater depletion in the middle east from GRACE with implications for transboundary water management in the Tigris–Euphrates–western Iran region." *Water Resour. Res.* 49 (2): 904–914. https://doi.org/10.1002/wrcr.20078.

Vrugt, J. A., and W. Bouten. 2002. "Validity of first-order approximations to describe parameter uncertainty in soil hydrologic models." *Soil Sci. Soc. Am. J.* 66 (6): 1740–1751. https://doi.org/10.2136/sssaj2002.1740.

Vu, M., S. V. Raghavan, and S. Y. Liong. 2012. "SWAT use of gridded observations for simulating runoff—A Vietnam river basin study." *Hydrol. Earth Syst. Sci.* 16 (8): 2801. https://doi.org/10.5194/hess-16-2801-2012.

Wible, T. 2014. "Enhanced watershed modeling and data analysis with a fully coupled hydrologic model and cloud-based flow analysis." Ph.D. thesis, Dept. of Civil and Environmental Engineering, Colorado State Univ.

Wilson, R. 2012. "Water-shortage crisis escalating in the Tigris–Euphrates basin." Future Directions International. Accessed August 28, 2012. http://www.futuredirections.org.au/publication/water-shortage-crisis-escalating-in-the-tigris-euphrates-basin/.

Xie, P., M. Chen, S. Yang, A. Yatagai, T. Hayasaka, Y. Fukushima, and C. Liu. 2007. "A gauge-based analysis of daily precipitation over east Asia." *J. Hydrometeorol.* 8 (3): 607–626. https://doi.org/10.1175/JHM583.1.

Xue, X., Y. Hong, A. S. Limaye, J. J. Gourley, G. J. Huffman, S. I. Khan, C. Dorji, and S. Chen. 2013. "Statistical and hydrological evaluation of TRMM-based multi-satellite precipitation analysis over the Wangchu basin of Bhutan: Are the latest satellite precipitation products 3B42V7 ready for use in ungauged basins?" *J. Hydrol.* 499: 91–99. https://doi.org/10.1016/j.jhydrol.2013.06.042.

Yang, D., X. Shi, and P. Marsh. 2015. "Variability and extreme of Mackenzie river daily discharge during 1973–2011." *Quat. Int.* 380: 159–168. https://doi.org/10.1016/j.quaint.2014.09.023.

Yang, J., P. Reichert, and K. C. Abbaspour. 2007a. "Bayesian uncertainty analysis in distributed hydrologic modeling: A case study in the Thur river basin (Switzerland)." *Water Resour. Res.* 43 (10): W10401. https://doi.org/10.1029/2006WR005497.

Yang, J., P. Reichert, K. C. Abbaspour, and H. Yang. 2007b. "Hydrological modelling of the Chaohe basin in China: Statistical model formulation and Bayesian inference." *J. Hydrol.* 340 (3): 167–182. https://doi.org/10.1016/j.jhydrol.2007.04.006.

Yatagai, A., K. Kamiguchi, O. Arakawa, A. Hamada, N. Yasutomi, and A. Kitoh. 2012. "APHRODITE: Constructing a long-term daily gridded precipitation dataset for Asia based on a dense network of rain gauges." *Bull. Am. Meteorol. Soc.* 93 (9): 1401–1415. https://doi.org/10.1175/BAMS-D-11-00122.1.

Yuan, F., L. Zhang, K. Win, L. Ren, C. Zhao, Y. Zhu, S. Jiang, and Y. Liu. 2017. "Assessment of GPM and TRMM multi-satellite precipitation products in streamflow simulations in a data-sparse mountainous watershed in Myanmar." *Remote Sens.* 9 (3): 302. https://doi.org/10.3390/rs9030302.

Zhu, Q., W. Xuan, L. Liu, and Y. P. Xu. 2016. "Evaluation and hydrological application of precipitation estimates derived from PERSIANN-CDR, TRMM 3B42V7, and NCEP-CFSR over humid regions in China." *Hydrol. Processes* 30 (17): 3061–3083. https://doi.org/10.1002/hyp.10846.